NUMERICAL SCHUBERT CALCULUS VIA THE LITTLEWOOD-RICHARDSON HOMOTOPY ALGORITHM

ANTON LEYKIN, ABRAHAM MARTÍN DEL CAMPO, FRANK SOTTILE, RAVI VAKIL, AND JAN VERSCHELDE

Abstract. We develop the Littlewood-Richardson homotopy algorithm, which uses numerical continuation to compute solutions to Schubert problems on Grassmannians and is based on the geometric Littlewood-Richardson rule. One key ingredient of this algorithm is our new optimal formulation of Schubert problems in local Stiefel coordinates as systems of equations. Our implementation can solve problem instances with tens of thousands of solutions.

The Schubert calculus on the Grassmannian [15] studies the linear subspaces that have specified positions with respect to fixed flags of linear spaces. This is a rich class of well-understood geometric problems that appear in applications such as the pole placement problem in linear systems theory [2, 3, 13, 35] and in information theory [1]. Schubert problems serve as a laboratory for investigating new phenomena in enumerative geometry, such as possible numbers of real solutions [5, 9, 26, 27, 33] or monodromy/Galois groups [18, 22, 29, 21]. While classical algorithms count the number of solutions [4], these applications drive a need to compute the actual solutions to Schubert problems.

General blackbox symbolic and numerical methods for solving systems of polynomial equations do not perform well on large Schubert problems, as they are not complete intersections. *Numerical Schubert calculus* consists of numerical algorithms adapted to the structure of Schubert problems. A homotopy algorithm is *optimal* when no solution path diverges for generic instances of the problem. The Pieri homotopy algorithm for solving special Schubert problems [11] is an optimal algorithm for Schubert calculus. That algorithm is based on a proof of Pieri's rule using geometric specializations [25]. It was implemented and refined [20, 33, 35], and has been used to compute feedback laws for linear systems [35] and to compute Galois groups of Schubert problems [18]. Special Schubert problems can be formulated as imposing simple rank-deficiency on several matrices of

2010 *Mathematics Subject Classification.* 14N15, 65H10.

Key words and phrases. Schubert Calculus, Grassmannian, Littlewood-Richardson Rule, Numerical Homotopy Continuation.

This project was supported by American Institute of Mathematics through their SQuaREs program.

Work of Leykin supported in part by the National Science Foundation under grant DMS-1719968.

Work of Martín del Campo supported in part by CONACyT under grant Cátedra-1076.

Work of Sottile supported in part by the National Science Foundation under grant DMS-1501370.

Work of Vakil supported in part by the National Science Foundation under grant DMS-1500334.

Work of Verschelde supported in part by the National Science Foundation under grants ACI-1440534 and DMS-1854513.

general linear forms. Specialized algorithms for solving simple rank-deficiency on a matrix with polynomial entries were recently developed in [8].

The more general Littlewood-Richardson rule was given a proof using geometric specializations organized by a combinatorial checkers game [30, 31]. This geometric rule leads to our main contribution, the first general Littlewood-Richardson homotopy algorithm. A preliminary study for this was carried out in [28] for some Schubert problems with a handful of solutions. The present work is far more intricate and the resulting algorithm is applicable to *any* Schubert problem on a Grassmannian. A novel feature is that in the homotopy, the underlying space and its parametrization change, but the equations do not. We have implemented the Littlewood-Richardson homotopy algorithm both in the `NumericalSchubertCalculus` package of `Macaulay2` [6] and in `PHCpack` [32]. Our software is free and open source, available on `github`, and capable of solving problems with tens of thousands of solutions, which are currently far out of reach for all other available methods.

Section 1 gives background on the Schubert calculus and numerical homotopy continuation. This includes a new formulation for Schubert varieties using the fewest possible number of equations. Section 2 describes the geometric Littlewood-Richardson rule, which is the foundation of our algorithm. Section 3 is the heart of the paper, for it describes the Littlewood-Richardson homotopy algorithm in detail. Section 4 gives some examples of what our software can compute. Details of the implementations will appear in [17].

1. Schubert Calculus and Homotopy Continuation

We describe Schubert problems and explain how they may be represented on a computer with an efficient set of equations. This is in terms of local Stiefel coordinates and exploits the Plücker embedding. We conclude with a discussion on numerical homotopy continuation. We will fix positive integers $k < n$ throughout.

1.1. Schubert problems.

The *Grassmannian* $\mathrm{Gr}(k,n)$ of k-planes in $\mathbb{C}^n$ is a complex manifold of dimension $k(n-k)$. It has Schubert subvarieties indexed by *brackets*, which are k-element subsets α of $[n] := \{1,\ldots,n\}$, written in increasing order $\alpha\colon \alpha_1 < \cdots < \alpha_k$. Write $\binom{[n]}{k}$ for the set of all brackets. A *flag* F is an increasing sequence of linear subspaces,

$$F\ :\ F_1\ \subset\ F_2\ \subset\ \cdots\ \subset\ F_n\ =\ \mathbb{C}^n\,,\qquad \text{with}\quad \dim F_i = i\,.$$

A bracket $\alpha \in \binom{[n]}{k}$ and a flag F determine a *Schubert variety*,

$$X_\alpha F\ :=\ \{H \in \mathrm{Gr}(k,n)\ \mid\ \dim(H \cap F_{\alpha_i}) \geq i \text{ for } i = 1,\ldots,k\}\,.$$

This variety has dimension $|\alpha| := \sum_{i=1}^k (\alpha_i - i)$ and its codimension in $\mathrm{Gr}(k,n)$ is $\|\alpha\| := k(n-k) - |\alpha|$.

The bracket $[3,4,7,8] \in \binom{8}{4}$ and a flag F in $\mathbb{C}^8$ determine the Schubert variety,

$$\begin{aligned} X_{[3,4,7,8]}F\ =\ \{H \in \mathrm{Gr}(4,8) \mid \dim H \cap F_3 \geq 1\,,\ \dim H \cap F_4 \geq 2\,,\\ \dim H \cap F_7 \geq 3\,,\ \text{and}\ \dim H \cap F_8 \geq 4\}\,. \end{aligned} \tag{1}$$

This subvariety of $\mathrm{Gr}(4,8)$ has dimension $12 = (3-1)+(4-2)+(7-3)+(8-4)$ and codimension $4 = 4\cdot(8-4) - 12$.

The geometric problems studied in Schubert calculus are given by lists of brackets $(\alpha^1,\ldots,\alpha^s)$ and flags $F^1,\ldots,F^s$, and involve understanding the set of k-planes in the intersection

$$X_{\alpha^1}F^1 \;\cap\; X_{\alpha^2}F^2 \;\cap\; \cdots \;\cap\; X_{\alpha^s}F^s\,. \tag{2}$$

When the flags $F^1,\ldots,F^s$ are general and the brackets satisfy $\|\alpha^1\|+\cdots+\|\alpha^s\| = k(n-k)$, this intersection (2) is zero-dimensional and transverse [14], and its number of points, $d(\alpha^1,\ldots,\alpha^s)$, does not depend on the flags. This number may be computed using combinatorial algorithms from the Schubert calculus [4]. A list of brackets $(\alpha^1,\ldots,\alpha^s)$ satisfying $\|\alpha^1\|+\cdots+\|\alpha^s\| = k(n-k)$ is a *Schubert problem*. An *instance* of that Schubert problem is given by flags $F^1,\ldots,F^s$, and its *solutions* are the points of the intersection (2).

The most basic Schubert problem is (α,β) where $\|\alpha\|+\|\beta\| = k(n-k)$. An instance is given by two general flags F, M. The intersection $X_\alpha F \cap X_\beta M$ is empty unless $\beta_{k+1-i} = n+1-\alpha_i$ for $i=1,\ldots,k$, and in that case it is the singleton,

$$X_\alpha F \cap X_\beta M \;=\; \Big\{\bigoplus_{i=1}^{k} F_{\alpha_i}\cap M_{n+1-\alpha_i}\Big\}\,. \tag{3}$$

As the flags F and M are in general position, $F_{\alpha_i}\cap M_{n+1-\alpha_i}$ is one-dimensional.

1.2. **Representing Schubert problems on a computer.** To solve a Schubert problem on a computer requires that it be formulated as a system of polynomial equations in some coordinates. There are several formulations, including global Plücker coordinates, local Stiefel coordinates, and more exotic primal-dual [7] or lifted [10] coordinates. An advantage of local Stiefel coordinates is that they involve the fewest variables.

An ordered basis $\mathbf{f}_1,\ldots,\mathbf{f}_n$ of $\mathbb{C}^n$ forms the columns of an invertible matrix in $\mathbb{C}^{n\times n}$ and vice-versa, with the standard basis corresponding to the identity matrix, I. Given such a basis/matrix, we obtain a flag whose i-dimensional subspace is the span of the columns $\mathbf{f}_1,\ldots,\mathbf{f}_i$. Therefore, two matrices F, F' correspond to the same flag if and only if there is an invertible upper triangular matrix T such that $F' = FT$. We use the same symbol for an invertible matrix and for the corresponding flag.

The *Stiefel manifold* is the set $\mathcal{M}_{k,n}$ of $n\times k$ matrices of full rank k. Taking column span leads to a map $\phi\colon \mathcal{M}_{k,n} \twoheadrightarrow \mathrm{Gr}(k,n)$ which is a principal $GL_k(\mathbb{C})$-bundle. This admits a (discontinuous) section given by putting any matrix in a fiber into reverse column reduced echelon form. The set $\mathcal{X}_\alpha$ of *echelon* matrices with pivots in rows α is isomorphic to $\mathbb{C}^{|\alpha|}$. Under ϕ, the set $\mathcal{X}_\alpha$ is isomorphic to a dense open subset of the Schubert variety $X_\alpha I$. For example, when $n=6$ and $k=3$, here are the sets $\mathcal{X}_\alpha$ for the brackets $\alpha=[4,5,6]$, $[2,4,6]$, and $[2,3,5]$, respectively, where x_{ij} indicates an indeterminate:

$$\begin{pmatrix} x_{11} & x_{12} & x_{13}\\ x_{21} & x_{22} & x_{23}\\ x_{31} & x_{32} & x_{33}\\ 1 & 0 & 0\\ 0 & 1 & 0\\ 0 & 0 & 1 \end{pmatrix} \qquad \begin{pmatrix} x_{11} & x_{12} & x_{13}\\ 1 & 0 & 0\\ 0 & x_{32} & x_{33}\\ 0 & 1 & 0\\ 0 & 0 & x_{53}\\ 0 & 0 & 1 \end{pmatrix} \qquad \begin{pmatrix} x_{11} & x_{12} & x_{13}\\ 1 & 0 & 0\\ 0 & 1 & 0\\ 0 & 0 & x_{43}\\ 0 & 0 & 1\\ 0 & 0 & 0 \end{pmatrix}$$

A set $\mathcal{Y} \subset \mathcal{M}_{k,n}$ will be called *Stiefel coordinates* for a subvariety Y of $\mathrm{Gr}(k,n)$, if there is an invertible matrix M such that $\phi(M\mathcal{Y})$ is dense in Y and the map $\phi \circ M \colon \mathcal{Y} \to Y$ is birational. Thus $\mathcal{X}_\alpha$ gives Stiefel coordinates for the Schubert variety $X_\alpha I$ and also for $X_\alpha M$. This definition allows the mild but useful ambiguity that for M invertible, both $\mathcal{X}_\alpha$ and $M\mathcal{X}_\alpha$ are Stiefel coordinates for both $X_\alpha I$ and for $X_\alpha M$.

Given a point $H \in \mathcal{M}_{k,n}$, the condition that the k-plane $\phi(H)$ lies in $X_\alpha F$ may be expressed in terms of the rank of augmented matrices,

$$\mathrm{rank}\,(\ H \ \mid\ F_{\alpha_i}\ ) \ \leq\ k{+}\alpha_i{-}i \qquad \text{for} \quad i = 1,\ldots,k\,. \tag{4}$$

Equivalently, for each $i = 1,\ldots,k$, all square $(k{+}\alpha_i{-}i{+}1) \times (k{+}\alpha_i{-}i{+}1)$ minors of the matrix $(H \mid F_{\alpha_i})$ vanish. This gives

$$\sum_{i=1}^{k} \binom{n}{k{+}\alpha_i{-}i{+}1}\binom{k{+}\alpha_i}{k{+}\alpha_i{-}i{+}1}$$

equations, which are polynomials in the entries of H with coefficients depending upon F. There are no minors when $\alpha_i = n{-}k{+}i$, and conditions are redundant if $\alpha_k = n$, or when $1{+}\alpha_i = \alpha_{i+1}$. For example, when $k = 4$, $n = 8$, and $\alpha = [3,4,7,8]$, the only meaningful condition in the definition (1) of $X_{[3,4,7,8]}F$ is $\dim H \cap F_4 \geq 2$, or equivalently $\mathrm{rank}(H \mid F_4) \leq 6$. This is given by the vanishing of the 64 non-maximal 7×7 minors of the 8×8 matrix $(H \mid F_4)$.

This discussion shows that we may model the intersection of a subset $Y \subset \mathrm{Gr}(k,n)$ with a collection of Schubert varieties,

$$Y\ \cap\ X_{\alpha^1}F^1\ \cap\ X_{\alpha^2}F^2\ \cap\ \cdots\ \cap\ X_{\alpha^s}F^s\,,$$

by first selecting a set $\mathcal{Y} \subset \mathcal{M}_{k,n}$ of Stiefel coordinates for Y and then generating the minors imposing the rank conditions (4), for each pair (α^i, F^i).

The Littlewood-Richardson Homotopy Algorithm (Algorithm 2 in Section 3.3) takes as input two positive integers $k < n$ indicating the Grassmannian $\mathrm{Gr}(k,n)$, brackets $\alpha^1,\ldots,\alpha^s$ representing a Schubert problem on $\mathrm{Gr}(k,n)$, and general flags $F^1,\ldots,F^s$ in $\mathbb{C}^n$. Given these, it computes all the solutions to the corresponding instance (2).

Theorem 1.1. *For any Schubert problem $(\alpha^1,\ldots,\alpha^s)$ and general flags $F^1,\ldots,F^s$, the Littlewood-Richardson Homotopy Algorithm finds all points in the intersection* (2).

The proof of Theorem 1.1 is included in the proof of correctness of the Littlewood-Richardson Homotopy Algorithm.

1.3. **Efficient representation of Schubert problems.** We formulate membership of a 4-plane in $X_{[3,4,7,8]}F$ in terms of the Stiefel manifold $\mathcal{M}_{4,8}$. The condition (4) on augmented matrices is $\mathrm{rank}(H \mid F_4) \leq 6$, where the 4-plane H is the column space of a 8×4 matrix

of indeterminates and we write the (constant) entries of the 8×4 matrix F as $*$s,

$$(H \mid F_4) \;=\; \left(\begin{array}{cccc|cccc} x_{11} & x_{12} & x_{13} & x_{14} & * & * & * & * \\ x_{21} & x_{22} & x_{23} & x_{24} & * & * & * & * \\ x_{31} & x_{32} & x_{33} & x_{34} & * & * & * & * \\ x_{41} & x_{42} & x_{43} & x_{44} & * & * & * & * \\ x_{51} & x_{52} & x_{53} & x_{54} & * & * & * & * \\ x_{61} & x_{62} & x_{63} & x_{64} & * & * & * & * \\ x_{71} & x_{72} & x_{73} & x_{74} & * & * & * & * \\ x_{81} & x_{82} & x_{83} & x_{84} & * & * & * & * \end{array}\right) .$$

The rank condition is given by the vanishing of the 64 non-maximal minors of $(H \mid F_4)$ obtained by deleting one row and one column. Half of these equations are homogeneous cubics and half are homogeneous quartics. The ideal of $X_{[3,4,7,8]}F$ in $\mathcal{M}_{4,8}$ is generated by only 16 cubic minors, but it is not clear *a priori* which 16 suffice. We present another formulation of this Schubert variety that involves only 17 linearly independent quartics.

The Plücker embedding $\mathrm{Gr}(k,n) \hookrightarrow \mathbb{P}(\wedge^k\mathbb{C}^n)$ is induced by the map $\mathrm{Mat}_{n\times k}(\mathbb{C}) \to \wedge^k\mathbb{C}^n$ given by the $\binom{n}{k}$ maximal minors of a matrix $H = (h_{i,j}) \in \mathrm{Mat}_{n\times k}(\mathbb{C})$

$$H \;\longmapsto\; \Bigl(p_\alpha(H) \;\mid\; \alpha \in \tbinom{[n]}{k}\Bigr) \;\in\; \bigwedge^k \mathbb{C}^n .$$

Here, $p_\alpha(H) := \det(h_{\alpha_i,j})_{i,j=1}^k$ is the determinant of the square submatrix consisting of the rows indexed by α in H. These minors $p_\alpha(H)$ are the *Plücker coordinates* of H. The image is $\mathrm{Gr}(k,n)$ and it is cut out by the quadratic Plücker relations [4, §9.1, Lemma 1].

The Schubert variety $X_\alpha I$ is cut out from $\mathrm{Gr}(k,n)$ by a subset of Plücker coordinates. Specifically, $H \in X_\alpha I$ if and only if $p_\beta(H) = 0$ for all $\beta \in \binom{[n]}{k}$ with $\beta \not\leq \alpha$. This may be seen as follows. Given a general matrix $H \in X_\alpha I$, the rank of the square submatrix formed by its rows $\beta_1, \ldots, \beta_k$ is k unless $\beta_i < \alpha_i$ for some i. This uses the partial order on the index set $\binom{[n]}{k}$ of brackets, defined by $\alpha \leq \beta \iff \alpha_i \leq \beta_i$ for $i = 1, \ldots, k$.

Example 1.2. When $n = 8$, $k = 4$, and $\alpha = [3,4,7,8]$, there are 17 brackets β with $\beta \not\leq \alpha$:

$$\begin{gathered} [5,6,7,8]\,,\ [4,6,7,8]\,,\ [3,6,7,8]\,,\ [4,5,7,8]\,,\ [2,6,7,8]\,,\ [3,5,7,8]\,,\ [4,5,6,8]\,, \\ [1,6,7,8]\,,\ [2,5,7,8]\,,\ [3,5,6,8]\,,\ [4,5,6,7]\,,\ [1,5,7,8]\,,\ [2,5,6,8]\,,\ [3,5,6,7]\,, \\ [1,5,6,8]\,,\ [2,5,6,7]\,,\ [1,5,6,7]\,. \end{gathered}$$ ◇

Observe that $H \in X_\alpha F$ if and only if $F^{-1}H \in X_\alpha I$ if and only if $p_\beta(F^{-1}H) = 0$ for all $\beta \not\leq \alpha$. Using the Cauchy-Binet formula, we can write

$$p_\beta(F^{-1}H) \;=\; \sum_{\gamma \in \binom{[n]}{k}} p_{\beta,\gamma}(F^{-1}) p_\gamma(H)\,,$$

where $p_{\beta,\gamma}(F^{-1}) := \det((F^{-1})_{\beta_i,\gamma_j})_{i,j=1}^k$ is the (β,γ)-th entry in the matrix $\wedge^k(F^{-1})$. We summarize this discussion with the following theorem.

Theorem 1.3 (**Efficient equations for** $Y \cap X_\alpha F$**).** *Let* $\mathcal{Y}$ *be Stiefel coordinates for* $Y \subset \mathrm{Gr}(k,n)$ *and compute the Plücker vector* $P(\mathcal{Y}) := (p_\beta(\mathcal{Y}) \mid \beta \in \binom{[n]}{k})$ *for* $\mathcal{Y}$*. Compute*

the rectangular matrix $P(\alpha)(F^{-1}) := (p_{\beta,\gamma}(F^{-1}) \mid \beta \not\leq \alpha,\, \gamma \in \binom{[n]}{k})$. *The entries in the matrix-vector product* $P(\alpha)(F^{-1}) \cdot P(\mathcal{Y})$ *cut out* $\phi(\mathcal{Y}) \cap X_\alpha F$ *from* $\phi(\mathcal{Y})$.

Remark 1.4. This method is even more efficient for the intersections of several Schubert varieties, as we only need to compute $P(\mathcal{Y})$ once. ◇

Remark 1.5. When this improvement was first implemented in our software, it resulted in speedups of several to 60-fold. For instance, for $\alpha = [3, 4, 7, 8]$, computing the problem $(\alpha, \alpha, \alpha, \alpha)$ with six solutions went from 20 minutes to 20 seconds. It is implemented in symbolic software used to study Galois groups in Schubert calculus [21]. ◇

1.4. **Numerical homotopy continuation.** A numerical homotopy continuation algorithm computes solutions to a system of polynomial equations by following known solutions to a different set of equations along a deformation (homotopy) between the two systems using predictor-corrector methods.

Suppose that we want to compute the solutions to a system

$$f_1(x_1, \ldots, x_m) \;=\; f_2(x_1, \ldots, x_m) \;=\; \cdots \;=\; f_M(x_1, \ldots, x_m) \;=\; 0 \tag{5}$$

of polynomial equations. A *homotopy* for (5) is a one-parameter family of equations $\mathcal{H}(x; t) = 0$ whose solutions at $t = 0$ are known and whose solutions at $t = 1$ include those of (5). Furthermore, restricting t to the interval $[0, 1]$ defines paths in $\mathbb{C}^m$ that connect the solutions of (5) from $t = 1$ to known solutions at $t = 0$.

For such a homotopy, standard predictor-corrector methods are used to numerically trace the known solutions at $t = 0$ to obtain solutions to (5) at $t = 1$ (see [23] for more details). The homotopy is *optimal* when every solution at $t = 0$ is connected to a unique solution to (5) at $t = 1$ along a path.

This procedure may be iterated, connecting one homotopy to another to solve (5) from known solutions to another system in two or more steps. The Pieri homotopy is such an optimal homotopy that used up to $k(n-k) - 2$ steps to solve special Schubert problems [11]. The Littlewood-Richardson homotopy (Algorithm 2 in Section 3.3) is also an optimal homotopy which solves more general Schubert problems on Grassmannians.

2. The Geometric Littlewood-Richardson Rule

The Littlewood-Richardson homotopy algorithm is based on the geometric Littlewood-Richardson rule [30]. It consists of a sequence of degenerations which successively transform an intersection $X_\alpha F \cap X_\beta M$ of Schubert varieties when F and M are general into a union of Schubert varieties $X_\gamma F$ where $\|\gamma\| = \|\alpha\| + \|\beta\|$.

These degenerations are encoded in the combinatorial checkerboard game, described in Section 2 of [30]. Subsection 2.18 of *loc. cit.* explains how these are combined into a checkerboard tournament that encodes the process of resolving a given Schubert problem. This checkerboard tournament forms the combinatorial backbone of the Littlewood-Richardson homotopy.

The intermediate components of the degenerations of intersections $X_\alpha F \cap X_\beta M$ are called checkerboard varieties; these are defined in Subsection 2.1, where we also describe

Stiefel coordinates for them. Subsection 2.2 describes the checkerboard game and explains how to combine several of them to get a checkerboard tournament.

2.1. **Checkerboard varieties.** We summarize salient features of [30, Sec. 2]. Given brackets α and β, the geometric Littlewood-Richardson rule is a sequence of $\binom{n}{2}+1$ families of subvarieties of $\mathrm{Gr}(k,n)$ parameterized by pairs of flags (F,M) in particular relative positions. The most general family is parameterized by pairs of flags in general position with the fiber over (F,M) being the intersection of Schubert varieties $X_\alpha F \cap X_\beta M$. In the least general family $M=F$ and the fiber over (F,F) is a union of Schubert varieties $X_\gamma F$ where $\|\gamma\| = \|\alpha\| + \|\beta\|$. In each intermediate family, the pair of flags (F,M) has a fixed non-general relative position and each fiber is a union of certain checkerboard varieties. These families fit together pairwise into $\binom{n}{2}$ families, transforming the intersection $X_\alpha F \cap X_\beta M$ into a union of Schubert varieties.

These $\binom{n}{2}+1$ families have the same base for any two brackets—each consists of all pairs (F,M) of flags having a fixed relative position encoded by a permutation π, where

$$\dim(M_i \cap F_j) \;=\; \#\{\ell \le j \mid \pi(\ell) \le i\}\,.$$

We encode the relative position between F and M in a *permutation array*, which is an $n \times n$ array of boxes with one black checker $\bullet$ in each row and column. We will refer to a permutation array by the corresponding permutation π, defined by the positions of the black checkers. For example, the permutation 356421 (given in one-line notation) corresponds to the following permutation array.

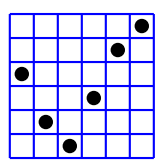

(6)

An ordered basis $\mathbf{m}_1,\ldots,\mathbf{m}_n$ for $\mathbb{C}^n$ and a permutation array π define flags F and M as follows. Identifying the checker in row i with $\mathbf{m}_i$, the i-plane M_i is the span of the checkers in the first i rows and the j-plane F_j is the span of the checkers in the first j columns. For example, for the permutation array (6), we have $M_3 = \langle \mathbf{m}_1, \mathbf{m}_2, \mathbf{m}_3\rangle$, while $F_3 = \langle \mathbf{m}_3, \mathbf{m}_5, \mathbf{m}_6\rangle$.

A *checkerboard* on a permutation array π is a placement $\bullet\bullet$ of k red checkers in π such that the red checkers are in distinct rows and columns, and any subset of j red checkers has at least j black checkers to its northwest ($\nwarrow$). Suppose that $\bullet\bullet$ is a checkerboard on a permutation array π and (F,M) is a pair of flags having relative position π given by an ordered basis $\mathbf{m}_1,\ldots,\mathbf{m}_n$ as above. For each subset S of red checkers, let $S(F,M)$ be the subspace of $\mathbb{C}^n$ spanned by the black checkers northwest of S.

Definition 2.1. The *checkerboard variety* $Y_{\bullet\bullet}(F,M) \subset \mathrm{Gr}(k,n)$ consists of all k-planes H such that $\dim H \cap S(F,M) \ge \#S$, for all subsets S of red checkers.

For the checkerboard $\bullet\bullet$ below, the checkerboard variety $Y_{\bullet\bullet}(F,M)$ is

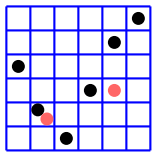

$$\begin{aligned} Y_{\bullet\bullet}(F,M) \;:=\; \{H \in \mathrm{Gr}(2,6) \mid & \dim H \cap \langle \mathbf{m}_3, \mathbf{m}_5\rangle \geq 1\,, \\ & \dim H \cap \langle \mathbf{m}_2, \mathbf{m}_3, \mathbf{m}_4\rangle \geq 1\,, \text{ and} \\ & H \subset \langle \mathbf{m}_2, \mathbf{m}_3, \mathbf{m}_4, \mathbf{m}_5\rangle\}\,. \end{aligned}$$

In [30], the checkerboard variety $Y_{\bullet\bullet}(F,M)$ is called a closed two-flag Schubert variety. In Lemma 2.6 *loc. cit.*, an open subset of $Y_{\bullet\bullet}(F,M)$ is described as a subset of a tower of projective bundles. This is equivalent to the following definition of Stiefel coordinates for a checkerboard variety.

Definition 2.2. Order the red checkers from top to bottom. The checkerboard variety $Y_{\bullet\bullet}(F,M)$ has Stiefel coordinates given by a set $\mathcal{Y}_{\bullet\bullet} = (y_{i,j})$ of reduced echelon matrices as follows. The entry $y_{i,j}$ is 0 when the black checker in row i is not northwest of the jth red checker, or if it is northwest and shares its square with a different red checker; the entry $y_{i,j}$ is a 1 if the jth red checker is in row i, and otherwise $y_{i,j}$ is an indeterminate.

The set $\phi(M\mathcal{Y}_{\bullet\bullet})$ is dense in the checkerboard variety $Y_{\bullet\bullet}(F,M)$. A k-plane $H \in \phi(M\mathcal{Y}_{\bullet\bullet})$ has a basis $\mathbf{h}_1,\ldots,\mathbf{h}_k$ where the vector

$$\mathbf{h}_j \;=\; \sum_{i=1}^{n} y_{i,j}\mathbf{m}_i\,,$$

corresponds to column j of $M\mathcal{Y}_{\bullet\bullet}$.

By Lemma 2.4 below, if there is a red checker northwest of red checker j, then it lies in the square of some (say the ith) black checker. We may use the column of this northwest red checker to reduce the column of the jth red checker in $\mathcal{Y}_{\bullet\bullet}$ so that the entry $y_{i,j}$ vanishes. Thus this entry must be zero for $\mathcal{Y}_{\bullet\bullet}$ to consist of echelon matrices.

Example 2.3. Figure 1 shows a checkerboard $\bullet\bullet$ and its Stiefel coordinates $\mathcal{Y}_{\bullet\bullet}$ when $n = 14$ and $k = 7$, with permutation array $\pi = (6,7,8,9,11,12,13,14,10,5,4,3,2,1)$. The entries 0 are forced by the requirement that the matrix be reduced echelon. The entries $\cdot$ are also 0 and they indicate that the black checker is not northwest of the corresponding red checker. The letters $A,\ldots,F,r$, and R and the arrows will be explained later. $\diamond$

2.2. **The checkerboard game.** The steps in the geometric Littlewood-Richardson rule, the deformations and degenerations of $X_\alpha F \cap X_\beta M$, and of subsequent checkerboard varieties, are all encoded in the combinatorial checkerboard game. We discuss its salient features, following [30, §§2.9–2.19].

The checkerboard game is a movement of black checkers that encodes the specialization of a pair (F,M) of general flags to the pair (F,F) in special position. The movement of the black checkers is a bubble sort beginning with the permutation ω_0, where $\omega_0(i) = n+1-i$, so that the black checkers will lie on the anti-diagonal. In the game, the black checkers remain in their respective columns, changing only rows. The first move interchanges the rows of the lowest (leftmost) two checkers.

For subsequent moves, note that the black checkers of a permutation π in mid-sort will be in one of four regions, illustrated in Figure 2: (A) the upper right portion of the

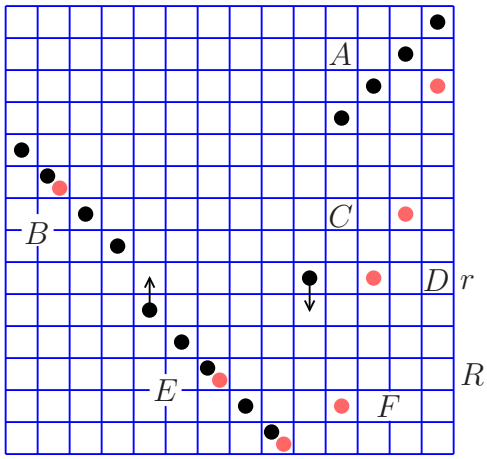

$$\begin{bmatrix} y_{1,1} & \cdot & \cdot & \cdot & \cdot & \cdot & \cdot \\ y_{2,1} & \cdot & y_{2,3} & \cdot & \cdot & \cdot & \cdot \\ 1 & \cdot & y_{3,3} & y_{3,4} & \cdot & \cdot & \cdot \\ \cdot & \cdot & y_{4,3} & y_{4,4} & \cdot & y_{4,6} & \cdot \\ \cdot & y_{5,2} & y_{5,3} & y_{5,4} & y_{5,5} & y_{5,6} & y_{5,7} \\ \cdot & 1 & 0 & 0 & 0 & 0 & 0 \\ \cdot & \cdot & 1 & y_{9,4} & y_{7,5} & y_{7,6} & y_{7,7} \\ \cdot & \cdot & \cdot & y_{8,4} & y_{8,5} & y_{8,6} & y_{8,7} \\ \cdot & \cdot & \cdot & 1 & \cdot & y_{9,6} & \cdot \\ \cdot & \cdot & \cdot & \cdot & y_{10,5} & y_{10,6} & y_{10,7} \\ \cdot & \cdot & \cdot & \cdot & y_{11,5} & y_{11,6} & y_{11,7} \\ \cdot & \cdot & \cdot & \cdot & 1 & 0 & 0 \\ \cdot & \cdot & \cdot & \cdot & \cdot & 1 & y_{13,7} \\ \cdot & \cdot & \cdot & \cdot & \cdot & \cdot & 1 \end{bmatrix}$$

FIGURE 1. Stiefel coordinates corresponding to a checkerboard.

anti-diagonal, (B) along a diagonal starting in the first column at the row below (A), (E) along a diagonal starting one column and two rows after (B), or there will be a solitary checker (D) in the column between (A) and (E) and in the row between (B) and (E). If there is no column between the checkers in (A) and those along a diagonal, then consider that diagonal as (E), that (B) is empty, and the solitary checker (D) is the last checker in (A). We call the solitary checker (D) the *descending checker* and the top checker in (E) the *ascending checker*. When $n = 4$, there are $7 = \binom{4}{2}+1$ permutation arrays in the bubble sort.

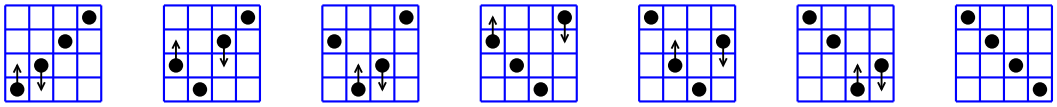

(7)

The subsequent permutation array is obtained by interchanging the rows of the descending and ascending checkers. Call the row of the descending checker the *critical row* and the diagonal (E) the *critical diagonal*. See Figure 2.

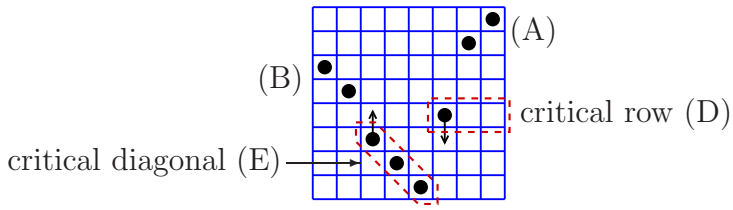

FIGURE 2. Critical row and critical diagonal.

The checkerboard game also constructs a tree with checkerboards as nodes. This tree is a ranked poset with $\binom{n}{2}+1$ ranks corresponding to the underlying permutation arrays. Its root encodes the intersection $X_\alpha F \cap X_\beta M$ as a checkerboard for the permutation array

ω_0, placing red checkers in positions $(\beta_{k+1-i}, \alpha_i)$ for $i = 1, \ldots, k$. When $n = 6$ and $k = 3$ with $\alpha = [2, 4, 6]$ and $\beta = [3, 4, 6]$, we have the following checkerboard $\bullet\bullet$ and Stiefel coordinates $\mathcal{Y}_{\bullet\bullet}$ for $X_\alpha F \cap X_\beta M$:

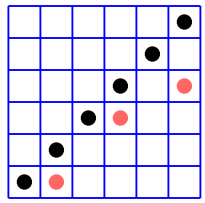

$$\begin{bmatrix} \cdot & \cdot & y_{13} \\ \cdot & \cdot & y_{23} \\ \cdot & y_{32} & 1 \\ \cdot & 1 & \cdot \\ y_{51} & \cdot & \cdot \\ 1 & \cdot & \cdot \end{bmatrix}.$$

If for some i, $\beta_{k+1-i} + \alpha_i < n$, then $X_\alpha F \cap X_\beta M = \emptyset$ and there is no checkerboard game.

Each node in this tree has one or two children according to which of nine cases it is in. These cases are determined by two questions, each of which has three answers.

Where is the top red checker in the critical diagonal (E)?

(0) In the square of the ascending black checker.
(1) Elsewhere in the critical diagonal.
(2) There is no red checker in the critical diagonal.

Where is the red checker in the critical row (D)?

(0) In the square of the descending black checker.
(1) Elsewhere in the critical row.
(2) There is no red checker in the critical row.

Table 1 shows the movement of the checkers in these nine cases. The rows correspond to the first question and the columns to the second question. Only the relevant part of each checkerboard is shown.

Table 1. Movement of red checkers.

	0	1	2
0			
1	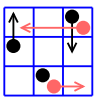	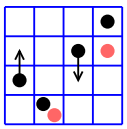 or 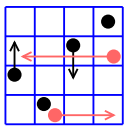	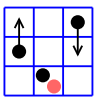
2			

In case $(1, 1)$ there are two possibilities, referred to as *stay* or *swap*, for in one the red checkers remain in place, while in the other they swap columns. The swap occurs only if there are no other red checkers in the rectangle between the two, called *blockers*. Figure 3 shows a blocker.

A red checker is in region A, B, or E if both its row and column contain black checkers in the corresponding region. Checkers in regions C, D, or F lie in the row of some black

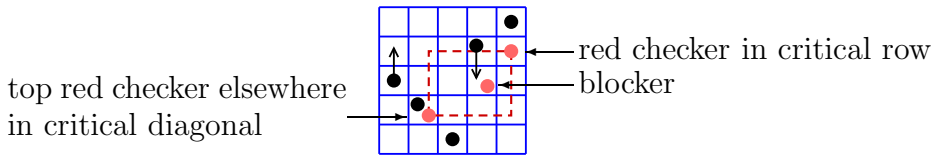

FIGURE 3. A blocker.

checker that is in region B, is descending, or is in region E, respectively, and they lie in a column of a black checker in A. It is helpful to refer to Figure 1.

Lemma 2.4. *In a checkerboard* $\bullet\bullet$*, each red checker strictly to the left of the column of the descending checker lies in the square of some black checker in region* B *or* E*. The other red checkers are arranged southwest to northeast in regions* F*,* D*,* C*, and* A*. In particular, if one red checker is northwest of another, then the first lies in the square of a black checker in region* B *or* E*.*

Proof. This is true in the initial position in the permutation array ω_0, and each move of Table 1 preserves this configuration. □

For a permutation π, let P_π be the space of pairs of flags (F, M) in relative position π. If π follows σ in the bubble sort, then in the space of pairs of flags, P_π lies in the closure of P_σ and is dense in a component of $\overline{P_\sigma} \smallsetminus P_\sigma$ so that $\overline{P_\pi}$ is a boundary divisor of $\overline{P_\sigma}$.

Suppose that $\bullet\bullet'$ is a checkerboard with permutation array σ and child checkerboard $\bullet\bullet$ with permutation array π (or $\bullet\bullet$ and $\bullet\bullet''$ are its two children in case $(1,1)$ with no blockers). Let Y be the family over $P_\pi \cup P_\sigma \subset \overline{P_\sigma}$ whose fiber over $(F, M) \in P_\sigma$ is the checkerboard variety $Y_{\bullet\bullet'}(F, M)$ and over $(F, M) \in P_\pi$ is the checkerboard variety $Y_{\bullet\bullet}(F, M)$ (or $Y_{\bullet\bullet}(F, M) \cup Y_{\bullet\bullet''}(F, M)$ in case (1,1)). Then Theorem 2.13 of [30] states that Y is the closure in $(P_\pi \cup P_\sigma) \times \mathrm{Gr}(k, n)$ of its restriction to P_σ.

At the conclusion of the checkerboard game, all checkers lie along the main diagonal. For such a checkerboard, the corresponding checkerboard variety is the Schubert variety $X_\gamma F$, where the red checkers lie in positions $(\gamma_1, \gamma_1), \ldots, (\gamma_k, \gamma_k)$.

Figure 4 shows the checkerboard game in the first nontrivial case when $n = 4$, $k = 2$ and $\alpha = \beta = [2, 4]$. It deforms $X_{[2,4]}F \cap X_{[2,4]}M$ into $X_{[1,4]}F \cup X_{[2,3]}F$. The arrows are

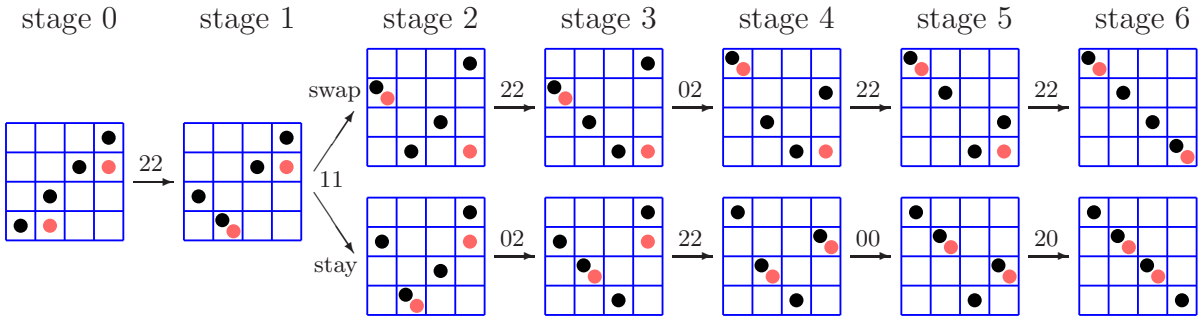

FIGURE 4. Resolving the intersection $X_{[2,4]}F \cap X_{[2,4]}M$.

labeled by the position of the move in Table 1. The geometry does not change in the

first step, as the 2-plane H continues to meet both $M_2 = \langle \mathbf{m}_1, \mathbf{m}_2 \rangle$ and $F_2 = \langle \mathbf{m}_3, \mathbf{m}_4 \rangle$ in a 1-dimensional subspace. In the second stage, H continues to meet both M_2 and F_2, but these now meet in $\langle \mathbf{m}_2 \rangle$. There are two possibilities for H as we are in case $(1,1)$ of Table 1. Either $\mathbf{m}_2 \in H$ (swap) or $H \subset \langle F_2, M_2 \rangle = \langle \mathbf{m}_1, \mathbf{m}_2, \mathbf{m}_4 \rangle$ (stay). In subsequent moves the vectors $\mathbf{m}_1, \ldots, \mathbf{m}_4$ rearrange themselves. Three dimensional pictures in [28, Figure 4] illustrate Figure 4[1].

A checkerboard game may have identical nodes. Since the children of a node depend only on the checkerboard of that node (and not on the previous history), we may identify identical nodes, obtaining a ranked *checkerboard poset* whose maximal elements (leaves) are indexed by a subset of those brackets γ with $\|\gamma\| = \|\alpha\| + \|\beta\|$.

Suppose that we have a Schubert problem, $(\beta^1, \beta^2, \ldots, \beta^s)$. The checkerboard poset for β^1, β^2 has leaves indexed by brackets α with $\|\alpha\| = \|\beta^1\| + \|\beta^2\|$. For each such α, we form the checkerboard poset for α, β^3 and attach it to the leaf labeled α. Identifying identical nodes in this new poset gives a poset whose leaves are indexed by brackets γ with $\|\gamma\| = \|\beta^1\| + \|\beta^2\| + \|\beta^3\|$. Repeating this process forms the *checkerboard tournament*, which is a poset having $s-2$ levels of checkerboard posets whose leaves are labeled by brackets δ with $\|\delta\| + \|\beta^s\| = k(n-k)$. We prune this poset, leaving only the single leaf labeled by the sequence $(\beta^s)^\vee := (n+1-\beta^s_k, \ldots, n+1-\beta^s_1)$. The number of solutions to the original Schubert problem is the number of saturated chains in this poset from the root to the unique leaf, by Corollary 2.17 and the discussion in Subsection 2.18 of [30].

3. The Littlewood-Richardson Homotopy

We first explain the Littlewood-Richardson homotopy conceptually. Given a Schubert problem $(\beta^1, \ldots, \beta^s)$ and flags $F, F^2, \ldots, F^s$, suppose that we know all the points of

$$X_\gamma F \;\cap\; X_{\beta^3} F^3 \;\cap\; \cdots \;\cap\; X_{\beta^s} F^s \tag{8}$$

for γ any index with $\|\gamma\| = \|\beta^1\| + \|\beta^2\|$. We use this to find all solutions to the instance of the Schubert problem

$$X_{\beta^1} F \;\cap\; X_{\beta^2} F^2 \;\cap\; X_{\beta^3} F^3 \;\cap\; \cdots \;\cap\; X_{\beta^s} F^s\,. \tag{9}$$

Formulating membership in $X_{\beta^3} F^3 \cap \cdots \cap X_{\beta^s} F^s$ as a system of polynomial equations, we use the geometric Littlewood-Richardson rule for $X_{\beta^1} F \cap X_{\beta^2} F^2$ to continue the points of (8) for all γ back to solutions to the instance (9) of the original Schubert problem.

Similarly, if for some ℓ, all solutions to instances of Schubert problems of the form

$$X_\gamma F \;\cap\; X_{\beta^\ell} F^\ell \;\cap\; \cdots \;\cap\; X_{\beta^s} F^s \tag{10}$$

are known for all γ with $\|\gamma\| + \|\beta^\ell\| + \cdots + \|\beta^s\| = k(n-k)$, then we may find all solutions to Schubert problems of the form

$$X_\alpha F \;\cap\; X_{\beta^{\ell-1}} F^{\ell-1} \;\cap\; X_{\beta^\ell} F^\ell \;\cap\; \cdots \;\cap\; X_{\beta^s} F^s\,, \tag{11}$$

for all α with $\|\alpha\| + \|\beta^{\ell-1}\| + \|\beta^\ell\| + \cdots + \|\beta^s\| = k(n-k)$. Thus starting with the (known) solution (3) to $X_{(\beta^s)^\vee} F \cap X_{\beta^s} F^s$, after $s-2$ iterations of this procedure we obtain all solutions to the original Schubert problem.

[1]Animations at `http://www.math.tamu.edu/~sottile/research/stories/vakil/4lines/1.html`

In passing from the Schubert problem (10) coming from a leaf of the checkerboard game for the pair $(\alpha, \beta^{\ell-1})$ to the problem corresponding to its root (11), we encounter *intermediate Schubert problems* corresponding to nodes $\bullet\bullet$ of the checkerboard game. An instance of the intermediate Schubert problem corresponding to the node $\bullet\bullet$ is an intersection

$$Y_{\bullet\bullet}(F, M) \;\cap\; X_{\beta^\ell} F^\ell \cap \cdots \cap X_{\beta^s} F^s \,. \tag{12}$$

Our algorithm requires 1-parameter families of flags to use in each step of the homotopy. We also need to specify how the equations are generated, and how the solutions obtained from one checkerboard game are passed to the next one in the tournament.

In Subsection 3.1 we describe the families of flags underlying each checkerboard game. In Subsection 3.2 we describe the coordinate homotopies, one for each pair of subsequent nodes in a checkerboard game. In Subsection 3.3 we explain how these fit together in the Littlewood-Richardson homotopy.

3.1. **Families of flags.** The Littlewood-Richardson homotopy uses the degenerations of the geometric Littlewood-Richardson rule along a sequence of one-parameter families of flags that form a skeleton of the families P_σ of Section 2.2. This begins with $\binom{n}{2}+1$ pairs (F, M) of flags in position π, one pair for each permutation π in the bubble sort. We also select $\binom{n}{2}$ explicit one-parameter families of pairs $(F'(t), M'(t))$ that connect these flags. The explicit choices we make here are those made in our software. The flags F and $F'(t)$ are fixed to be the standard coordinate flag, so we only need to specify the flags M and $M'(t)$ for each permutation and family. These have the following property. If M' corresponds to the permutation σ and M to the next permutation π in the bubble sort, then the family $M'(t)$ connecting them satisfies

$$M'(0) \;=\; M \qquad \text{and} \qquad M'(1) \;=\; M' \,, \tag{13}$$

and for all $t \neq 0$, the pair $(F, M'(t))$ has position σ.

The subspace F_i of F is spanned by the ith column of the identity matrix. At a permutation π, the flag M is given by an ordered basis $\mathbf{m}_1, \ldots, \mathbf{m}_n$ so that M_i is spanned by $\mathbf{m}_1, \ldots, \mathbf{m}_i$ while F_i is spanned by $\mathbf{m}_{\pi(1)}, \ldots, \mathbf{m}_{\pi(i)}$, but $\mathbf{m}_1, \ldots, \mathbf{m}_n$ is not necessarily a permutation of the columns of the identity matrix. This is illustrated in the second row of Figure 5.

At the leaves of a checkerboard game, $M = F$. We describe the other flags recursively. Suppose that the flag M corresponds to a permutation π in the bubble sort with σ the previous permutation, and let r be the critical row in the sort from σ to π. Then the flag M' corresponding to σ is given by the basis $\mathbf{m}'_1, \ldots, \mathbf{m}'_n$, where

$$\mathbf{m}'_i \;=\; \mathbf{m}_i \quad \text{for } i \neq r, r{+}1 \,, \qquad \mathbf{m}'_r \;=\; \mathbf{m}_r - \mathbf{m}_{r+1} \,, \qquad \text{and} \qquad \mathbf{m}'_{r+1} \;=\; \mathbf{m}_r \,. \tag{14}$$

For $t \neq 0$, the family $M'(t)$ is given by the basis $\mathbf{m}'_1(t), \ldots, \mathbf{m}'_n(t)$, where

$$\begin{aligned} \mathbf{m}'_i(t) \;&=\; \mathbf{m}_i \;=\; \mathbf{m}'_i \qquad i \neq r, r{+}1 \,, \\ \mathbf{m}'_r(t) \;&=\; \mathbf{m}_r - t\mathbf{m}_{r+1} \;=\; t\mathbf{m}'_r + (1-t)\mathbf{m}'_{r+1} \,, \qquad \text{and} \\ \mathbf{m}'_{r+1}(t) \;&=\; \mathbf{m}_r \;=\; \mathbf{m}'_{r+1} \,. \end{aligned} \tag{15}$$

For $t \neq 0$, we have $\langle \mathbf{m}'_r(t), \mathbf{m}'_{r+1}(t)\rangle = \langle \mathbf{m}_r, \mathbf{m}_{r+1}\rangle$. As $\lim_{t\to 0} M'(t) = M$, we set $M(0) := M$. The flag M at the root corresponds to the triangular matrix $(m_{i,j})$, where

$$m_{i,j} \;=\; \begin{cases} 0 & \text{if } n < j+i \\ (-1)^i & \text{otherwise.} \end{cases}$$

Figure 5 shows the permutations, arrays, matrices M, and families $M'(t)$ when $n = 4$.

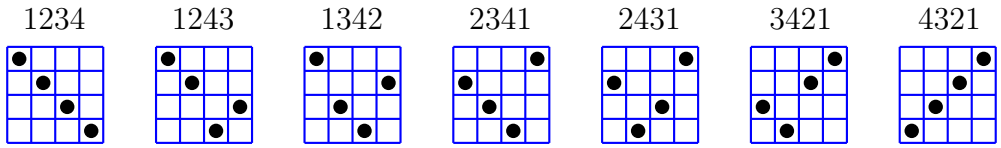

$$M \quad \begin{matrix} 1&0&0&0\\ 0&1&0&0\\ 0&0&1&0\\ 0&0&0&1 \end{matrix} \qquad \begin{matrix} 1&0&0&0\\ 0&1&0&0\\ 0&0&1&1\\ 0&0&-1&0 \end{matrix} \qquad \begin{matrix} 1&0&0&0\\ 0&1&1&0\\ 0&-1&0&1\\ 0&1&0&0 \end{matrix} \qquad \begin{matrix} 1&1&0&0\\ -1&0&1&0\\ 1&0&0&1\\ -1&0&0&0 \end{matrix} \qquad \begin{matrix} 1&1&0&0\\ -1&0&1&1\\ 1&0&-1&0\\ -1&0&0&0 \end{matrix} \qquad \begin{matrix} 1&1&1&0\\ -1&-1&0&1\\ 1&1&0&0\\ -1&0&0&0 \end{matrix} \qquad \begin{matrix} 1&1&1&1\\ -1&-1&-1&0\\ 1&1&0&0\\ -1&0&0&0 \end{matrix}$$

$$M'(t) \quad \begin{matrix} 1&0&0&0\\ 0&1&0&0\\ 0&0&1&1\\ 0&0&-t&0 \end{matrix} \qquad \begin{matrix} 1&0&0&0\\ 0&1&1&0\\ 0&-t&0&1\\ 0&t&0&0 \end{matrix} \qquad \begin{matrix} 1&1&0&0\\ -t&0&1&0\\ t&0&0&1\\ -t&0&0&0 \end{matrix} \qquad \begin{matrix} 1&1&0&0\\ -1&0&1&1\\ 1&0&t&0\\ -1&0&0&0 \end{matrix} \qquad \begin{matrix} 1&1&1&0\\ -1&-t&0&1\\ 1&t&0&0\\ -1&0&0&0 \end{matrix} \qquad \begin{matrix} 1&1&1&1\\ -1&-1&-t&0\\ 1&1&0&0\\ -1&0&0&0 \end{matrix}$$

FIGURE 5. Permutation arrays, matrices M, and families of matrices $M(t)$.

3.2. **Stiefel coordinates and homotopy for checkerboard moves.** Suppose that the permutation σ is followed by π in the bubble sort. Fix, as in Subsection 3.1, the flags F, M, M', and $M'(t)$. Let $\bullet\circ'$ be a checkerboard with permutation array σ and suppose that $\bullet\circ$ is a child checkerboard of $\bullet\circ'$ with permutation array π. Then by Theorem 2.3 of [30] the family of checkerboard varieties $Y_{\bullet\circ'}(F, M'(t))$ for $t \neq 0$ extends to a family $Y_{\bullet\circ,\bullet\circ'}(t)$ over $\mathbb{C}$ with $Y_{\bullet\circ}(F, M)$ a component of the special fiber at $t = 0$. (If $\bullet\circ$ is the unique child checkerboard of $\bullet\circ'$, then $Y_{\bullet\circ}(F, M)$ is the special fiber, otherwise there is a second component $Y_{\bullet\circ''}(F, M)$ corresponding to the other child $\bullet\circ''$.)

The key construction in the Littlewood-Richardson homotopy is a set of Stiefel coordinates $\mathcal{Y}_{\bullet\circ}(t)$ for this family, in the following sense.

(i) $\mathcal{Y}_{\bullet\circ}(0)$ are Stiefel coordinates for $Y_{\bullet\circ}(F, M)$ in that $\phi(M\mathcal{Y}_{\bullet\circ}(0))$ is dense in the checkerboard variety $Y_{\bullet\circ}(F, M) = Y_{\bullet\circ}(F, M(0))$.

(ii) For $t \neq 0$, we have that $\phi(M\mathcal{Y}_{\bullet\circ}(t))$ is dense in $Y_{\bullet\circ'}(F, M(t))$.

Thus $\mathcal{Y}_{\bullet\circ}(t)$ gives Stiefel coordinates for the family $Y_{\bullet\circ'}(F, M(t))$, parameterizing an open subset that meets the component $Y_{\bullet\circ}(F, M)$ of the special fiber. These coordinates $\mathcal{Y}_{\bullet\circ}(t)$ will be defined below and their properties verified.

Remark 3.1. If $\bullet\circ'$ has another child $\bullet\circ''$, then $\mathcal{Y}_{\bullet\circ''}(t)$ also gives Stiefel coordinates for $Y_{\bullet\circ'}(F, M(t))$ and $\phi(M\mathcal{Y}_{\bullet\circ''}(t))$ meets the component $Y_{\bullet\circ''}(F, M)$ of the special fiber. $\diamond$

These Stiefel coordinates $\mathcal{Y}_{\bullet\circ}(t)$ are used to generate a homotopy corresponding to the edge $\bullet\circ$–$\bullet\circ'$ in the checkerboard tournament. We describe this homotopy.

Algorithm 1 (Checkerboard Homotopy Algorithm)

Let $(\gamma, \beta^{\ell-1}, \beta^{\ell}, \cdots, \beta^{s})$ be a Schubert problem and suppose that $\bullet\circ$–$\bullet\circ'$ is an edge in the checkerboard game for $(\gamma, \beta^{\ell-1})$ with $\bullet\circ'$ the parent of $\bullet\circ$.

Input: A solution y^* to the instance of the intermediate problem

$$Y_{\bullet\bullet}(F, M) \;\cap\; X_{\beta^\ell}F^\ell \;\cap\; \cdots \;\cap\; X_{\beta^s}F^s$$

represented as a matrix $(y^*_{i,j}) \in \mathcal{Y}_{\bullet\bullet}$ such that $y^* = \phi(M(y^*_{i,j}))$.

Output: The solution y' to the instance of the intermediate problem

$$Y_{\bullet\bullet'}(F, M') \;\cap\; X_{\beta^\ell}F^\ell \;\cap\; \cdots \;\cap\; X_{\beta^s}F^s \tag{16}$$

connected to y^* by the family $Y_{\bullet\bullet,\bullet\bullet'}(t)$ for $t \in [0,1]$, which is represented by a matrix $(y'_{i,j}) \in \mathcal{Y}_{\bullet\bullet'}$ with $y' = \phi(M'(y'_{i,j}))$.

1: Generate the coordinates $\mathcal{Y}_{\bullet\bullet}(t)$ for $Y_{\bullet\bullet,\bullet\bullet'}(t)$.

2: The homotopy $\mathcal{H}(y;t)$ is given by the equations of Theorem 1.3 for membership in the Schubert varieties $X_{\beta^\ell}F^\ell, \ldots, X_{\beta^s}F^s$ evaluated on the Stiefel coordinates $M\mathcal{Y}_{\bullet\bullet}(t)$.

3: Use numerical continuation to follow the homotopy $\mathcal{H}(y;t)$ from the the start solution $(y^*_{i,j})$ at $t = 0$ to a solution $(y^*_{i,j}(1))$ at $t = 1$.

4: Solve the equation

$$M'(\tilde{y}_{i,j}) \;=\; M(y^*_{i,j}(1)) \tag{17}$$

for the matrix $(\tilde{y}_{i,j})$.

5: Put the solution $(\tilde{y}_{i,j})$ in echelon form to get a point $(y'_{i,j}) \in \mathcal{Y}_{\bullet\bullet'}$.

Proof of correctness. The coordinates $\mathcal{Y}_{\bullet\bullet}(t)$ satisfy the properties (i) and (ii) above and thus $M\mathcal{Y}_{\bullet\bullet}$ gives Stiefel coordinates for the family $Y_{\bullet\bullet,\bullet\bullet'}(t)$. It follows that this homotopy computes a point y' in the target intermediate problem (16).

The arguments in Cases I–III below show that the echelon form of a solution to (17) lies in the Stiefel coordinates $\mathcal{Y}_{\bullet\bullet'}$, which completes the proof. □

Remark 3.2. In passing from π to σ, the black checkers in rows r and $r+1$ switch rows,

$$\pi \;:\; \begin{array}{|c|c|c|}\hline \bullet & \cdots & \\ \hline & \cdots & \bullet \\ \hline \end{array} \qquad \text{becomes} \qquad \sigma \;:\; \begin{array}{|c|c|c|}\hline & \cdots & \bullet \\ \hline \bullet & \cdots & \\ \hline \end{array}\,.$$

If M is the flag for π and M' the flag for σ, then by (14), $\mathbf{m}'_{r+1} = \mathbf{m}_r$ and $\mathbf{m}'_r = \mathbf{m}_r - \mathbf{m}_{r+1}$. Thus the basis element corresponding to the left moving black checker is unchanged, while that corresponding to the right moving black checker is changed, but their span is unchanged. It follows that if there is no red checker in the critical row r, then the geometric condition on the k-plane is unchanged in the move. ◇

As there are ten different checkerboard moves in Table 1, there are potentially ten different families of Stiefel coordinates $\mathcal{Y}_{\bullet\bullet}$ for the family $Y_{\bullet\bullet,\bullet\bullet'}(t)$. Analyzing their geometry reveals there are only three geometrically distinct cases for the construction of $\mathcal{Y}_{\bullet\bullet}(t)$. We indicate these cases by their positions in the 3×3 array of Table 1,

$$\text{I} \;:\; \begin{array}{|c|c|c|}\hline & & \text{x} \\ \hline & & \text{x} \\ \hline & & \text{x} \\ \hline \end{array}\,, \qquad \text{II} \;:\; \begin{array}{|c|c|c|}\hline & & \\ \hline & \text{stay} & \\ \hline \text{x} & \text{x} & \\ \hline \end{array}\,, \qquad \text{and} \qquad \text{III} \;:\; \begin{array}{|c|c|c|}\hline \text{x} & \text{x} & \\ \hline \text{x} & \text{swap} & \\ \hline & & \\ \hline \end{array}\,,$$

and refer to them by the numerals I, II, and III in the sequel.

Case I. There is no red checker in the critical row, so the geometric condition on the k-plane does not change, as noted in Remark 3.2. We need only to explain how to transform

the coordinates $\mathcal{Y}_{\bullet\circ}$ of a given k-plane into the coordinates $\mathcal{Y}_{\bullet\circ'}$ so that

$$M'\mathcal{Y}_{\bullet\circ'} \;=\; M\mathcal{Y}_{\bullet\circ}\,. \tag{18}$$

(*cf.* (17).) Write $y'_{i,j}$ and $y_{i,j}$ for the entry in row i and column j of $\mathcal{Y}_{\bullet\circ'}$ and $\mathcal{Y}_{\bullet\circ}$ respectively, and let r be the critical row. If we set

$$y'_{i,j} \;:=\; y_{i,j} \;\; i\neq r,r{+}1\,, \quad y'_{r,j} \;:=\; -y_{r+1,j}\,, \quad \text{and} \quad y'_{r+1,j} \;:=\; y_{r,j}+y_{r+1,j}\,, \tag{19}$$

then (18) is satisfied as

$$\begin{aligned} y_{r,j}\mathbf{m}_r + y_{r+1,j}\mathbf{m}_{r+1} &= y_{r,j}\mathbf{m}'_{r+1} + y_{r+1,j}(\mathbf{m}'_{r+1}-\mathbf{m}'_r)\\ &= -y_{r+1,j}\mathbf{m}'_r \;+\; (y_{r,j}+y_{r+1,j})\mathbf{m}'_{r+1}\\ &= y'_{r,j}\mathbf{m}'_r \;+\; y'_{r+1,j}\mathbf{m}'_{r+1}\,. \end{aligned}$$

In practice, our software solves the equation (18) for the entries of $\mathcal{Y}_{\bullet\circ'}$.

If there is a red checker in row $r{+}1$ of $\bullet\circ'$, then its column will not be in echelon form in $\mathcal{Y}_{\bullet\circ'}$: If its column index is j, then the last two non-zero entries are in rows r and $r{+}1$, and they are $y'_{r,j}=-1$ and $y'_{r+1,j}=1+y_{r,j}$. In this case, we divide that column by $y'_{r+1,j}$ to put $\mathcal{Y}_{\bullet\circ'}$ into (reduced) echelon form, as we do in our software.

Case II. As there is a checker in the critical row, by Remark 3.2, the geometric condition on the k-plane changes and the Stiefel coordinates $\mathcal{Y}_{\bullet\circ}(t)$ will involve t. We describe them and then prove they have the properties claimed. We will write $j\in A,B$ to indicate that the jth red checker of $\bullet\circ$ is in region A or in region B, and the same for the other regions or rows of the checkerboard as defined in Figure 1.

Let $(y_{i,j})=\mathcal{Y}_{\bullet\circ}$ be the Stiefel coordinates from Definition 2.2. Define $\mathcal{Y}_{\bullet\circ}(t)=(y_{i,j}(t))$, by setting $y_{i,j}(t):=y_{i,j}$ if $i\neq r{+}1$. When $i=r{+}1$, set $y_{r+1,j}(t):=y_{r+1,j}=0$ if $j\in E$, and otherwise set

$$y_{r+1,j}(t) \;:=\; y_{r+1,j} \;-\; ty_{r,j}\,. \tag{20}$$

Observe that if $j\in A,B$, or C, then its row is above r so that $y_{r+1,j}=y_{r,j}=y_{r+1,j}(t)=0$. Note that $y_{r+1,j}(t)$ is non-zero when $j\in F$ or when j lies in row r, for when j lies in row r, $y_{r,j}=1$ and $y_{r+1,j}=0$.

Lemma 3.3. *For any $t\neq 0$, $\phi(M\mathcal{Y}_{\bullet\circ}(t))$ is dense in the checkerboard variety $Y_{\bullet\circ'}(F,M'(t))$ and $\phi(M\mathcal{Y}_{\bullet\circ}(0))$ is dense in $Y_{\bullet\circ}(F,M'(0))$.*

Proof. When $t=0$, this holds as $\mathcal{Y}_{\bullet\circ}(0)=\mathcal{Y}_{\bullet\circ}$, $M\mathcal{Y}_{\bullet\circ}$ gives Stiefel coordinates for $Y_{\bullet\circ}(F,M)$, and $M'(0)=M$. For $t\neq 0$, we will show that if we solve the equation $M'(t)\mathcal{Y}_{\bullet\circ'}(t)=M\mathcal{Y}_{\bullet\circ}(t)$ for the $n\times k$ matrix $\mathcal{Y}_{\bullet\circ'}(t)$, then $\mathcal{Y}_{\bullet\circ'}(t)$ for $t\neq 0$ is a curve in $\mathcal{Y}_{\bullet\circ'}$ whose entries are functions of $y_{i,j}$ and t.

Let $\mathbf{h}_1(t),\ldots,\mathbf{h}_k(t)$ be the column vectors of $M\mathcal{Y}_{\bullet\circ}(t)$, which span the k-plane $\phi(M\mathcal{Y}_{\bullet\circ}(t))$. If $j\in E$, then

$$\mathbf{h}_j(t) \;=\; \sum_{i\neq r,r+1} y_{i,j}\mathbf{m}_i \;+\; y_{r,j}\mathbf{m}_r \;+\; 0\cdot\mathbf{m}_{r+1}\,,$$

as $y_{r+1,j}=0$. If $j\notin E$, then by (20),

$$\mathbf{h}_j(t) \;=\; \sum_{i\neq r,r+1} y_{i,j}\mathbf{m}_i \;+\; y_{r,j}\mathbf{m}_r \;+\; (y_{r+1,j}-ty_{r,j})\mathbf{m}_{r+1}\,.$$

Let us express $\mathbf{h}_i(t)$ in the basis $\mathbf{m}'_1(t),\ldots,\mathbf{m}'_n(t)$. If $i\neq r,r{+}1$, then by (15), $\mathbf{m}'_i(t)=\mathbf{m}_i$, and we have $\mathbf{m}'_r(t)=\mathbf{m}_r-t\mathbf{m}_{r+1}$ and $\mathbf{m}'_{r+1}(t)=\mathbf{m}_r$, so that when $t\neq 0$, we have

$$\mathbf{m}_{r+1} \;=\; \tfrac{1}{t}(\mathbf{m}'_{r+1}(t) \;-\; \mathbf{m}'_r(t))\,.$$

If $j\in E$, we have

$$\mathbf{h}_j(t) \;=\; \sum_{i\neq r,r+1} y_{i,j}\mathbf{m}'_i(t) \;+\; y_{r,j}\mathbf{m}'_{r+1}(t)\,.$$

If $j\notin E$, then

$$\mathbf{h}_j(t) \;=\; \sum_{i\neq r,r+1} y_{i,j}\mathbf{m}'_i(t) \;+\; (y_{r,j}-\tfrac{1}{t}y_{r+1,j})\mathbf{m}'_r(t) \;+\; \tfrac{1}{t}y_{r+1,j}\mathbf{m}'_{r+1}(t)\,.$$

Define the Stiefel coordinates $\mathcal{Y}_{\bullet\bullet'}(t)=(y'_{i,j}(t))$ for $t\neq 0$ by

$$y'_{i,j}(t) \;=\; y_{i,j} \quad \text{for} \quad i\neq r,r{+}1\,,$$

and if $j\in E$, then

$$y'_{r,j}(t) \;=\; 0 \;=\; y_{r+1,j} \qquad \text{and} \qquad y'_{r+1,j}(t) \;=\; y_{r,j}\,,$$

and if $j\notin E$, then

$$y'_{r,j}(t) \;=\; y_{r,j} \;-\; \tfrac{1}{t}y_{r+1,j} \qquad \text{and} \qquad y'_{r+1,j}(t) \;=\; \tfrac{1}{t}y_{r+1,j}\,.$$

A consequence of these definitions is that for $t\neq 0$, the column vectors of $M'(t)\mathcal{Y}_{\bullet\bullet'}(t)$ are equal to $\mathbf{h}_1(t),\ldots,\mathbf{h}_k(t)$. That is,

$$M'(t)\mathcal{Y}_{\bullet\bullet'}(t) \;=\; M\mathcal{Y}_{\bullet\bullet}(t)\,.$$

Note that the entry $y'_{i,j}(t)$ is 0, 1, or an affine polynomial in the $y_{p,q}$ and $\frac{1}{t}$ if and only if the corresponding entry in the Stiefel coordinates $\mathcal{Y}_{\bullet\bullet'}$ of Definition 2.2 is 0, 1, or an indeterminate, respectively. This proves the lemma. □

Case III. This case is the most subtle. Let $\bullet\bullet$ be a child of $\bullet\bullet'$ with the checkerboard move in Case III in which two red checkers move columns. Let $(y_{i,j})$ be the entries in $\mathcal{Y}_{\bullet\bullet}$, as given in Definition 2.2. Let s be the index of the red checker in the critical row r, and $s{+}1$ the index of the other moving red checker, which is in row $R\geq r{+}1$.

Figure 6 gives an example of $\bullet\bullet$ and $\mathcal{Y}_{\bullet\bullet}$, which is a child of the checkerboard $\bullet\bullet'$ of Figure 1 with coordinates $\mathcal{Y}_{\bullet\bullet'}$, where the move connecting them is the swap move in the center of Table 1. Comparing these two figures will help to explain our arguments. In Figure 6, we have $s=4$, the red checker s is to the left in row $r=9$, and the red checker $s{+}1$ is to the right in row $R=12$. These two are in different columns in Figure 1.

We define $\mathcal{Y}_{\bullet\bullet}(t)=(y_{i,j}(t))$. The entry $y_{i,j}(t)$ will depend on the position of the red checker j. Recall that the black checkers are in regions A, B, E, or in row r.

(1) If $j\neq s$, set $y_{i,j}(t):=y_{i,j}$.
(2) When $j=s$, set $y_{r,s}(t):=y_{r+1,s+1}$ and $y_{r+1,s}(t):=-ty_{r+1,s+1}$, and

$$\begin{aligned} y_{a,s}(t) &:= -ty_{a,s+1} && \text{for } a\in A,\\ y_{b,s}(t) &:= y_{r+1,s+1}\cdot y_{b,s} && \text{for } b\in B, \end{aligned}$$

and if $e\in E\smallsetminus\{r{+}1\}$, then $y_{e,s}(t)=0=y_{e,s}$, as s is in row $r<e$.

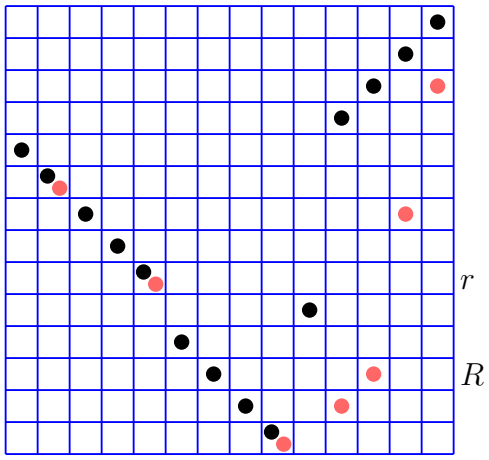

$$\begin{bmatrix} y_{1,1} & \cdot & \cdot & \cdot & \cdot & \cdot & \cdot \\ y_{2,1} & \cdot & y_{2,3} & \cdot & \cdot & \cdot & \cdot \\ 1 & \cdot & y_{3,3} & \cdot & y_{3,5} & \cdot & \cdot \\ \cdot & \cdot & y_{4,3} & \cdot & y_{4,5} & y_{4,6} & \cdot \\ \cdot & y_{5,2} & y_{5,3} & y_{5,4} & y_{5,5} & y_{5,6} & y_{5,7} \\ \cdot & 1 & 0 & 0 & 0 & 0 & 0 \\ \cdot & \cdot & 1 & y_{7,4} & y_{7,5} & y_{7,6} & y_{7,7} \\ \cdot & \cdot & \cdot & y_{8,4} & y_{8,5} & y_{8,6} & y_{8,7} \\ \cdot & \cdot & \cdot & 1 & 0 & 0 & 0 \\ \cdot & \cdot & \cdot & \cdot & y_{10,5} & y_{10,6} & \cdot \\ \cdot & \cdot & \cdot & \cdot & y_{11,5} & y_{11,6} & y_{11,7} \\ \cdot & \cdot & \cdot & \cdot & 1 & y_{12,6} & y_{12,7} \\ \cdot & \cdot & \cdot & \cdot & \cdot & 1 & y_{13,7} \\ \cdot & \cdot & \cdot & \cdot & \cdot & \cdot & 1 \end{bmatrix}$$

FIGURE 6. Stiefel coordinates corresponding to a checkerboard.

The terms $-ty_{a,s+1}$ for $a \in A$ occur only if the red checker s in the critical row in $\bullet\bullet'$ is not in the square of the descending checker.

Observe that $M\mathcal{Y}_{\bullet\bullet}$ is equal to $M\mathcal{Y}_{\bullet\bullet}(t)$, except in column s, and that if $\mathbf{h}_s$ and $\mathbf{h}_s(t)$ are the vectors of column s in $M\mathcal{Y}_{\bullet\bullet}$ and in $M\mathcal{Y}_{\bullet\bullet}(t)$ respectively, then

$$\mathbf{h}_s(t) \;=\; y_{r+1,s+1}\mathbf{h}_s \;-\; t\Big(y_{r+1,s+1}\mathbf{m}_{r+1} + \sum_{a\in A} y_{a,s+1}\mathbf{m}_a\Big)\,, \tag{21}$$

where the term inside the parentheses is a sum of components of the column vector $\mathbf{h}_{s+1}$.

Lemma 3.4. *For any $t \neq 0$, $\phi(M\mathcal{Y}_{\bullet\bullet}(t))$ is dense in the checkerboard variety $Y_{\bullet\bullet'}(F, M'(t))$ and $\phi(M\mathcal{Y}_{\bullet\bullet}(0))$ is dense in $Y_{\bullet\bullet}(F, M'(0))$.*

Proof. Note that $\mathcal{Y}_{\bullet\bullet}(0) = \mathcal{Y}_{\bullet\bullet}$, except in their sth columns. These columns are proportional, as $y_{i,s}(0) = y_{r+1,s+1} \cdot y_{i,s}$, for all i. This proves the statement for $t = 0$.

For $t \neq 0$, we show that $\phi(M\mathcal{Y}_{\bullet\bullet}(t))$ is dense in the checkerboard variety $Y_{\bullet\bullet'}(F, M'(t))$ by describing Stiefel coordinates $\mathcal{Y}_{\bullet\bullet'}(t) = (y'_{i,j}(t))$ with $\phi(M\mathcal{Y}_{\bullet\bullet}(t)) = \phi(M'(t)\mathcal{Y}_{\bullet\bullet'}(t))$ that have the following properties:

The transformation $\mathcal{Y}_{\bullet\bullet}(t) \to \mathcal{Y}_{\bullet\bullet'}(t)$ is invertible, and the entry $y'_{i,j}(t)$ of $\mathcal{Y}_{\bullet\bullet'}(t)$ is 1, 0, or a function of the $y_{p,q}$ and t if and only if the entry in the Stiefel coordinates $\mathcal{Y}_{\bullet\bullet'}$ of Definition 2.2 is 1, 0, or an indeterminate, respectively. (22)

Let $\mathbf{h}_1(t), \ldots, \mathbf{h}_k(t)$ be the k column vectors of $M\mathcal{Y}_{\bullet\bullet}(t)$. We use these to define the entries $y'_{i,j}(t)$ of $\mathcal{Y}_{\bullet\bullet'}(t)$, which depend upon the position of the red checker j in $\bullet\bullet'$. Recall from Figure 1 that red checkers in $\bullet\bullet'$ lie in one of the regions A–F.

If the red checker j is in a row above r, so that $j \in A$, B, or C, then

$$\mathbf{h}_j(t) \;=\; \sum_{i\in A,B} y_{i,j}\mathbf{m}_i \;=\; \sum_{i\in A,B} y_{i,j}\mathbf{m}'_i(t)\,. \tag{23}$$

If $j = s$, then we have

$$\mathbf{h}_s(t) \;=\; \sum_{a\in A} -ty_{a,s+1}\mathbf{m}_a \;+\; y_{r+1,s+1}\Big(\sum_{b\in B} y_{b,s}\mathbf{m}_b \;+\; \mathbf{m}_r - t\mathbf{m}_{r+1}\Big)\,. \tag{24}$$

If $j = s{+}1$, so that the red checker is in row R,

$$\mathbf{h}_{s+1}(t) \;=\; \sum_{a\in A} y_{a,s+1}\mathbf{m}_a \;+\; \sum_{b\in B} y_{b,s+1}\mathbf{m}_b \;+\; \sum_{e\in E\smallsetminus\{R\}} y_{e,s+1}\mathbf{m}_e \;+\; \mathbf{m}_R\,. \tag{25}$$

When $R = r{+}1$, the last sum is empty, and the last term is $\mathbf{m}_{r+1}$. Also, we always have $y_{r,s+1} = 0$ as the red checker s lies in the square of black checker r, which is northwest of red checker $s{+}1$.

For all other red checkers j, either $j \in F$ or $j \in E \smallsetminus \{R\}$, and $\mathbf{h}_j(t) \;=\; \sum_{i=1}^n y_{i,j}\mathbf{m}_i$. Note that $y_{r,j} = 0$ as red checker s lies in the square of black checker r, and both are northwest of red checker j. For $j \in E \smallsetminus \{R\}$, we have $y_{r+1,j} = 0$ as black checker $r{+}1$ is east of red checker j.

To define $y'_{i,j}(t)$, recall that $\mathbf{m}'_r(t) = \mathbf{m}_r - t\mathbf{m}_{r+1}$, $\mathbf{m}'_{r+1}(t) = \mathbf{m}_r$, and $\mathbf{m}'_i(t) = \mathbf{m}_i$ for $i \neq r, r{+}1$. If $j \in A$, B, or C, then by (23), we may define $y'_{i,j}(t) = y_{i,j}$, for then

$$\mathbf{h}_j(t) \;=\; \sum_{i=1}^n y'_{i,j}(t)\mathbf{m}'_i(t)\,. \tag{26}$$

As checkers above row r do not move, the entries $y'_{i,j}(t)$ for these j have the properties (22).

For $j = s$, we rewrite (24) in terms of $\mathbf{m}'_i(t)$ to get

$$\mathbf{h}_s(t) \;=\; \sum_{a\in A} -ty_{a,s+1}\mathbf{m}'_a(t) \;+\; y_{r+1,s+1}\Big(\sum_{b\in B} y_{b,s}\mathbf{m}'_b(t) \;+\; \mathbf{m}'_r(t)\Big)\,.$$

Define $y'_{r,s}(t) = 1$, $y'_{b,s}(t) = y_{b,s}$ for $b \in B$, $y'_{a,s}(t) = -t \cdot y_{a,s+1}/y_{r+1,s+1}$ for $a \in A$, and $y'_{i,s}(t) = 0$ for $i \in E$. With these definitions, we have

$$\mathbf{h}_s(t) \;=\; y_{r+1,s+1} \cdot \Big(\sum_{i=1}^n y'_{i,s}(t)\mathbf{m}'_i(t)\Big)\,, \tag{27}$$

so that (26) holds (up to the factor $y_{r+1,s+1}$) for $j = s$. Also, (22) holds as in $\bullet\bullet'$ red checker s lies in the same column as red checker $s{+}1$ in $\bullet\bullet$, and thus below the same black checkers in A as red checker $s{+}1$.

For $j = s{+}1$, replace $\mathbf{h}_{s+1}(t)$ by $\mathbf{h}'_{s+1}(t) := \mathbf{h}_{s+1}(t) + \frac{1}{t}\mathbf{h}_s(t)$. Note that both $\mathbf{h}_s(t), \mathbf{h}_{s+1}(t)$ and $\mathbf{h}_s(t), \mathbf{h}'_{s+1}(t)$ have the same span. By (24) and (25), this cancels the sums involving A and the terms involving $\mathbf{m}_{r+1}$. Its form is slightly different in the two cases $R > r{+}1$ and $R = r{+}1$. When $R > r{+}1$, $\mathbf{h}'_{s+1}(t)$ becomes

$$\sum_{b\in B}(\tfrac{1}{t}y_{r+1,s+1} \cdot y_{b,s} + y_{b,s+1})\mathbf{m}_b \;+\; \tfrac{1}{t}y_{r+1,s+1}\mathbf{m}_r \;+\; \sum_{e\in E\smallsetminus\{r+1,R\}} y_{e,s+1}\mathbf{m}_e \;+\; \mathbf{m}_R\,.$$

When $R = r{+}1$, we have $y_{r+1,s+1} = 1$ and $\mathbf{h}'_{s+1}(t)$ is

$$\sum_{b\in B}(\tfrac{1}{t}y_{b,s} + y_{b,s+1})\mathbf{m}_b \;+\; \tfrac{1}{t}\mathbf{m}_r\,.$$

Let $y'_{r+1,s+1}(t)$ be the coefficient of $\mathbf{m}_r = \mathbf{m}'_{r+1}(t)$ in these expressions and for $i \neq r{+}1$, let $y'_{i,s+1}(t)$ be the coefficient of $\mathbf{m}_i = \mathbf{m}'_i(t)$. As $\mathbf{m}'_r(t)$ does not appear, (26) holds for $j = s{+}1$, and these functions $y'_{i,s+1}(t)$ satisfy the properties (22).

We illustrate these definitions of $\mathbf{h}_s(t), \mathbf{h}_{s+1}(t)$, and $\mathbf{h}'_s(t)$ for the checkerboard $\bullet\bullet$ of Figure 6. Below are the columns s and $s{+}1$ of the Stiefel coordinates $\mathcal{Y}_{\bullet\bullet}(t)$, which correspond to the vectors $\mathbf{h}_s(t)$ and $\mathbf{h}_{s+1}(t)$, and a column corresponding to the $\mathbf{h}'_{s+1}(t)$.

$$\begin{bmatrix} \cdot & \cdot & \cdot \\ \cdot & \cdot & \cdot \\ -ty_{3,5} & y_{3,5} & \cdot \\ -ty_{4,5} & y_{4,5} & \cdot \\ y_{10,5}y_{5,4} & y_{5,5} & y_{5,5} + \frac{1}{t}y_{10,5}y_{5,4} \\ \cdot & \cdot & \cdot \\ y_{10,5}y_{7,4} & y_{7,5} & y_{7,5} + \frac{1}{t}y_{10,5}y_{7,4} \\ y_{10,5}y_{8,4} & y_{8,5} & y_{8,5} + \frac{1}{t}y_{10,5}y_{8,4} \\ y_{10,5} & \cdot & \frac{1}{t}y_{10,5} \\ -ty_{10,5} & y_{10,5} & \cdot \\ \cdot & y_{11,5} & y_{11,5} \\ \cdot & 1 & 1 \\ \cdot & \cdot & \cdot \\ \cdot & \cdot & \cdot \\ \mathbf{h}_s(t) & \mathbf{h}_{s+1}(t) & \mathbf{h}'_{s+1}(t) \end{bmatrix} \tag{28}$$

In the remaining cases, $j \in E \smallsetminus \{R\}$ and $j \in F$, the rows of the 0 entries in those columns of $\mathcal{Y}_{\bullet\bullet}$ and $\mathcal{Y}_{\bullet\bullet'}$ are different. For example, in $\mathcal{Y}_{\bullet\bullet}$ the entries in row R are indeterminates, while they are 0 in $\mathcal{Y}_{\bullet\bullet'}$. This is because the red checker $s{+}1$ in row R is not in the square of the black checker in $\bullet\bullet$, but it is in that square in $\bullet\bullet'$. This is observed in Figure 6, where the entry $y_{12,6} \neq 0$, but it is zero in Figure 1. To obtain this zero entry in $\mathcal{Y}_{\bullet\bullet'}(t)$, we use $\mathbf{h}'_{s+1}(t)$ to reduce $\mathbf{h}_j(t)$.

If $j \in E \smallsetminus \{R\}$, note that $y_{r,j} = 0 = y'_{r,j}$. Indeed, in $\bullet\bullet$, the red checker s lies in the square of black checker r, while in $\bullet\bullet'$, the black checker r is northeast of the red checker j. Also, $y_{r+1,j} = 0$, as the black checker $r{+}1$ is northeast of the red checker j in $\bullet\bullet$. Set $\mathbf{h}'_j(t) := \mathbf{h}_j(t) - y_{R,j}\mathbf{h}'_{s+1}(t)$. When $R = r{+}1$, $y_{R,j} = 0$ so $\mathbf{h}'_j(t) = \mathbf{h}_j(t)$, and otherwise

$$\mathbf{h}'_j(t) \;=\; \sum_{i\in B,E\smallsetminus\{R\}} (y_{i,j} - y_{R,j}\cdot y'_{i,s+1}(t))\mathbf{m}'_i(t) \;-\; y_{R,j}\cdot y'_{r+1,s+1}(t)\mathbf{m}'_{r+1}(t)\,.$$

Let $y'_{i,j}(t)$ be the coefficient of $\mathbf{m}'_i(t)$ in this expression. Since red checker j is in a row ρ below red checker $s{+}1$, $y'_{\rho,s+1}(t) = 0$ so $y'_{\rho,j}(t) = 1$. Also note that $y'_{r+1,j}(t) = -y_{R,j}\cdot y'_{r+1,s+1}(t)$ and $y'_{R,j}(t) = 0$, by construction.

If $j \in F$, then the differences between $\mathcal{Y}_{\bullet\bullet}$ and $\mathcal{Y}_{\bullet\bullet'}$ are that $y_{r,j} = y'_{R,j} = 0$ and both $y_{R,j}$ and $y'_{r,j}$ are indeterminates. We observe this in column six in Figures 1 and 6. Suppose that $R > r{+}1$. Then

$$\mathbf{h}_j(t) \;=\; \sum_{i\in A,B,E\smallsetminus\{r+1,R\}} y_{i,j}\mathbf{m}_i \;+\; y_{r+1,j}\mathbf{m}_{r+1} \;+\; y_{R,j}\mathbf{m}_R\,.$$

Set $\mathbf{h}'_j(t) := \mathbf{h}_j(t) - y_{R,j}\mathbf{h}'_{s+1}(t)$, which is

$$\sum_{a\in A} y_{a,j}\mathbf{m}_a \;+\; \sum_{i\in B,E\smallsetminus\{r+1,R\}} (y_{i,j} - y_{R,j}\cdot y'_{i,s+1}(t))\mathbf{m}_i \;-\; \tfrac{1}{t}y_{R,j}y_{r+1,s+1}\mathbf{m}_r \;+\; y_{r+1,j}\mathbf{m}_{r+1}\,.$$

To rewrite this in terms of $\mathbf{m}'_i(t)$, by (15) $\mathbf{m}_r = \mathbf{m}'_{r+1}(t)$, $\mathbf{m}_{r+1} = \frac{1}{t}(\mathbf{m}'_{r+1}(t) - \mathbf{m}'_r(t))$, and otherwise $\mathbf{m}_i = \mathbf{m}'_i(t)$, which gives

$$\begin{aligned}\mathbf{h}'_j(t) \;=\; \sum_{a\in A} y_{a,j}\mathbf{m}'_a(t) \;+\; &\sum_{i\in B,E\smallsetminus\{r+1,R\}} (y_{i,j} - y_{R,j}\cdot y'_{i,s+1}(t))\mathbf{m}'_i(t)\\ &-\; \tfrac{1}{t}y_{r+1,j}\mathbf{m}'_r(t) \;+\; \tfrac{1}{t}(y_{r+1,j} - y_{R,j}y_{r+1,s+1})\mathbf{m}'_{r+1}(t)\,.\end{aligned}$$

Let $y'_{i,j}(t)$ be the coefficient of $\mathbf{m}'_i(t)$ in this expression. This expression shows that (22) holds when $R > r{+}1$.

The argument is simpler when $R = r{+}1$, for then

$$\mathbf{h}_j(t) \;=\; \sum_{i\in A,B,E\smallsetminus\{r+1\}} y_{i,j}\mathbf{m}_i \;+\; y_{r+1,j}\mathbf{m}_{r+1}\,.$$

and so $\mathbf{h}'_j(t) := \mathbf{h}_j(t) - y_{r+1,j}\mathbf{h}'_{s+1}(t)$ is

$$\sum_{a\in A} y_{a,j}\mathbf{m}_a(t) \;+\; \sum_{i\in B,E\smallsetminus\{r+1\}} (y_{i,j} - y_{r+1,j}\cdot y'_{i,s+1}(t))\mathbf{m}_i(t)\,.$$

Let $y'_{i,j}(t)$ be the coefficient of $\mathbf{m}'_i(t)$ in this expression. Then

$$\mathbf{h}'_j(t) \;=\; \sum_{i=1}^{n} y'_{i,j}(t)\mathbf{m}'_i(t)\,,$$

and these functions $y'_{i,j}(t)$ satisfy the properties (22). □

Remark 3.5. In this proof, when $t \neq 0$ and for $j = s{+}1$, $j \in F$, or $j \in E \smallsetminus \{R\}$, we replaced $\mathbf{h}_j(t)$ by $\mathbf{h}'_j(t) = \mathbf{h}_j(t) - z\mathbf{h}'_\ell(t)$ where $\ell < j$ and z is the coefficient of $\mathbf{m}'_i(t)$ in $\mathbf{h}_j(t)$ and $\mathbf{m}'_i(t)$ is the leading term in $\mathbf{h}'_\ell(t)$ (with coefficient 1). In all these cases, this put the vectors $\mathbf{h}_1(t), \ldots, \mathbf{h}_k(t)$ into reduced echelon form with respect to the basis $M'(t)$. The content of the proof was that the resulting matrix $\mathcal{Y}_{\bullet\bullet'}(t)$ of coefficients satisfies the properties (22). Our software automatically performs this reduction to change coordinates from $\mathcal{Y}_{\bullet\bullet}(1)$ to $\mathcal{Y}_{\bullet\bullet'}(1) = \mathcal{Y}_{\bullet\bullet'}$ for the node $\bullet\bullet'$. ◇

Remark 3.6. The formulation in Case III can lead to numerical instability in computation. From (21), $\mathbf{h}_s(t)$ (column s in $M\mathcal{Y}_{\bullet\bullet}(t)$) is obtained by multiplying $\mathbf{h}_s$ (column s in $M\mathcal{Y}_{\bullet\bullet}$) by $y_{r+1,s+1}$ and subtracting part of column $s{+}1$ in $M\mathcal{Y}_{\bullet\bullet}$ multiplied by t. (See also (27) and the first column of the matrix (28), where $y_{r+1,s+1} = y_{10,5}$.) This leads to numerical instability in a computation when $y_{r+1,s+1}$ is close to zero. ◇

3.3. **Littlewood-Richardson Homotopy Algorithm.** Using the definitions and results of the previous subsections, including Algorithm 1, we describe the Littlewood-Richardson Homotopy Algorithm.

Let F be the flag in $\mathbb{C}^n$ corresponding to the identity matrix, and let M be the opposite flag. This corresponds to the permutation array for ω_0 and the matrix J with 1s along its anti-diagonal. These flags are at the root of each checkerboard game. Fix a Schubert problem $(\beta^1,\ldots,\beta^s)$ for $\mathrm{Gr}(k,n)$ and consider its checkerboard tournament $\mathcal{T}$. Every node in $\mathcal{T}$ is a checkerboard $\bullet\!\bullet$ and has an intermediate Schubert problem (12), for flags $F^\ell,\ldots,F^s$ which will be determined in the algorithm. The checkerboard game of such a node lies in level $\ell{-}2$ of $\mathcal{T}$.

Algorithm 2 Littlewood-Richardson Homotopy Algorithm

Input: An instance of a Schubert problem in $\mathrm{Gr}(k,n)$ given by two positive integers $k<n$, a list of brackets $(\beta^1,\ldots,\beta^s)$ such that $\|\beta^1\|+\cdots+\|\beta^s\| = k(n{-}k)$, and flags $E^1,\ldots,E^s$ represented by invertible $n\times n$ matrices.

Output: All solutions to the instance

$$X_{\beta^1}E^1 \;\cap\; \cdots \;\cap\; X_{\beta^s}E^s\,, \tag{29}$$

represented in Stiefel coordinates as $n\times k$ matrices.

Generate random upper unitriangular $n\times n$ matrices $A_3,\ldots,A_s$.

Compute the checkerboard tournament $\mathcal{T}$ for $\beta^1,\ldots,\beta^s$.

Populate each node $\bullet\!\bullet$ of $\mathcal{T}$ with an empty list of solutions and with flags

$$F^\ell \;:=\; A_\ell J\,,\; F^{\ell+1} \;:=\; A_\ell A_{\ell+1}J\,,\;\ldots\,,\; F^s \;:=\; A_\ell A_{\ell+1}\cdots A_s J\,, \tag{30}$$

where $\bullet\!\bullet$ lies in a checkerboard game at level $\ell-2$ of $\mathcal{T}$, and the corresponding intermediate Schubert problem is (12). Mark the node as as `'unresolved'`.

Populate the leaf of the last checkerboard game with the single solution (3) to

$$X_{(\beta^s)^\vee}F \cap X_{\beta^s}A_sJ$$

represented in Stiefel coordinates as the echelon form of the submatrix of A_s consisting of its columns $n{+}1{-}\beta^s_i$ for $i=1,\ldots,k$. Mark this node as `'resolved'`.

while Node $\bullet\!\bullet'$ of $\mathcal{T}$ is unresolved **do**
  if any child of $\bullet\!\bullet'$ is unresolved **then**
    replace $\bullet\!\bullet'$ by this child and return.
  end if
  if all children of $\bullet\!\bullet'$ are resolved **then**
    for each child $\bullet\!\bullet$ of $\bullet\!\bullet'$ **do**
      if $\bullet\!\bullet'$ is a leaf of a checkerboard game at level $\ell{-}2$ **then**
        $\bullet\!\bullet$ is the root of a game at level $\ell{-}1$.
        for all solutions $y=(y_{i,j})$ in node $\bullet\!\bullet$ **do**
          append $A_\ell(y_{i,j})$ to the list of solutions in $\bullet\!\bullet'$.
        end for
      else if $\bullet\!\bullet$ is a child of $\bullet\!\bullet'$ in the same checkerboard game as $\bullet\!\bullet'$ **then**
        for all solutions y of node $\bullet\!\bullet$ **do**

18: Use Algorithm 1 to obtain the corresponding solution y'
19: Append y' to the list of solutions for $\bullet\circ'$.
20: **end for**
21: **end if**
22: **end for**
23: **end if**
24: **end while**
25: When all nodes of $\mathcal{T}$ are resolved, the solutions at its root are all solutions to the instance

$$X_{\beta^1}F \;\cap\; X_{\beta^2}J \;\cap\; X_{\beta^3}(A_3J) \;\cap\; \cdots \;\cap\; X_{\beta^s}(A_3A_4\cdots A_sJ)\,.$$

Replace each solution y at the root by E^1y, producing all solutions to the instance of this Schubert problem given by the flags $E^1 = E^1F, (E^1J), (E^1A_3J), \ldots$.
26: Create a homotopy between these flags and the user-defined flags $E^1, E^2, \ldots, E^s$ and follow these points E^1y along that homotopy, to obtain all solutions to the user's instance (29).

Proof of correctness. We prove that the algorithm performs as described when the input flags $E^1, \ldots, E^s$ are general. This will also prove Theorem 1.1. Every node $\bullet\circ'$ in the checkerboard tournament corresponds to an intermediate Schubert problem

$$Y_{\bullet\circ'}(F, M') \;\cap\; X_{\beta^\ell}F^\ell \;\cap\; \cdots \;\cap\; X_{\beta^s}F^s\,, \tag{31}$$

where $\bullet\circ'$ is a node in a checkerboard game at level $\ell-2$ in $\mathcal{T}$ and the flags $F^\ell, \ldots, F^s$ are as defined by (30). Let $S(\bullet\circ')$ be the set of solutions to this intermediate Schubert problem (31). We claim that, when a node $\bullet\circ'$ is resolved in Algorithm 2, the set of solutions in that node (as constructed in Steps 10–22) equals $S(\bullet\circ')$, recorded in the Stiefel coordinates $\mathcal{Y}_{\bullet\circ'}$ of Subsection 2.1. Establishing this claim, as well as the arguments presented below about Steps 25 and 26, will complete the proof of correctness of Algorithm 2.

For any checkerboard $\bullet\circ$, the Stiefel coordinates $\mathcal{Y}_{\bullet\circ}$ parameterize only a dense subset of a checkerboard variety $Y_{\bullet\circ}(F, M)$. Our arguments below ignore this distinction. To validate them, note that for each checkerboard the points of the checkerboard variety $Y_{\bullet\circ}(F, M)$ that are not parameterized by $\mathcal{Y}_{\bullet\circ}$ form a proper subset, Z. As the flags F^i are general, Kleiman's Theorem [14] asserts that there will be no points of (31) that lie in Z. As there are only finitely many checkerboards, the choice of general flags F^i and E^i will guarantee that the algorithm computes all solutions to (29).

We prove the claim by induction on $\mathcal{T}$. The claim holds at the leaf of $\mathcal{T}$, by construction: Step 4 places the unique solution of the intermediate problem of the leaf (explained at the end of Subsection 1.1), and marks that node as resolved.

Suppose that $\bullet\circ'$ is a node of $\mathcal{T}$ that is not the leaf of any checkerboard game in $\mathcal{T}$. Then either $\bullet\circ'$ has a unique child $\bullet\circ$ or possibly two, $\bullet\circ$ and $\bullet\circ''$, in that checkerboard game. Before node $\bullet\circ'$ is resolved, its child node(s) must be resolved. By the induction hypothesis, Algorithm 2 has populated $\bullet\circ$ with the solutions $S(\bullet\circ)$ to its intermediate problem, and the same for $\bullet\circ''$ if it exists. The points $S'(\bullet\circ')$ used by Algorithm 2 to populate the node $\bullet\circ'$ are obtained from the solutions in $S(\bullet\circ)$ (and $S(\bullet\circ'')$) using

Algorithm 1, which follows them along the homotopy induced by the family $M\mathcal{Y}_{\bullet\circ}(t)$ (or $M\mathcal{Y}_{\bullet\circ''}(t)$).

In the geometric Littlewood-Richardson rule, these families are Stiefel coordinates for the family $Y_{\bullet\circ,\bullet\circ'}(t)$ for $t \in \mathbb{C}$ with fiber $Y_{\bullet\circ'}(F, M')$ over $t = 1$ and fiber $Y_{\bullet\circ}(F, M)$ (or $Y_{\bullet\circ}(F, M) \cup Y_{\bullet\circ''}(F, M)$) over $t = 0$. This implies that $S'(\bullet\circ')$ is the set of solutions to the intermediate problem at the node $\bullet\circ'$.

We prove the claim when $\bullet\circ'$ is a leaf of a checkerboard game. Such a leaf has only one child in the tournament $\mathcal{T}$, which is the root of the subsequent checkerboard game. In this case, there is a bracket γ such that the intermediate problems at these two nodes are

$$\bullet\circ' \qquad X_\gamma F \,\cap\, X_{\beta^\ell} F^\ell \,\cap\, \cdots \,\cap\, X_{\beta_s} F^s \tag{32}$$

$$\bullet\circ \qquad X_\gamma F \,\cap\, X_{\beta^\ell} J \,\cap\, X_{\beta^{\ell+1}} \widetilde{F}^{\ell+1} \,\cap\, \cdots \,\cap\, X_{\beta_s} \widetilde{F}^s\,, \tag{33}$$

where the flags $F^\ell, \ldots, F^s$ are defined by (30), as are the flags $\widetilde{F}^{\ell+1}, \ldots, \widetilde{F}^s$, except that the index ℓ of the ambient checkerboard poset changes, so that

$$\widetilde{F}^{\ell+1} \;=\; A_{\ell+1} J\,,\; \widetilde{F}^{\ell+2} \;=\; A_{\ell+1} A_{\ell+2} J\,,\; \ldots\,,\; \widetilde{F}^s \;=\; A_{\ell+1} \cdots A_s J\,.$$

Since $A_\ell F$ and F give the same flag, the intersection (32) is obtained from that of (33) through left multiplication by A_ℓ. Thus if $\bullet\circ$ is resolved and populated by the points $S(\bullet\circ)$ in the intersection (33), then Steps 13–15 of Algorithm 2 populate node $\bullet\circ'$ with all the points $S(\bullet\circ')$ in the intersection (32), completing the proof of the claim.

The argument for Step 25, going from the root of $\mathcal{T}$, is that the intermediate Schubert problem passes from

$$X_{\beta_1} F \,\cap\, X_{\beta_2} J \,\cap\, X_{\beta_3} F^3 \,\cap\, \cdots \,\cap\, X_{\beta_s} F^s$$

to

$$X_{\beta_1} E^1 \,\cap\, X_{\beta_2} E^1 J \,\cap\, X_{\beta_3} E^1 F^3 \,\cap\, \cdots \,\cap\, X_{\beta_s} E^1 F^s \tag{34}$$

which is the same as passing between leafs and roots in the proof of the claim. Finally, Step 26 is simply applying a parameter homotopy [19, 24] between the solutions to (34) and those of the original Schubert problem

$$X_{\beta_1} E^1 \,\cap\, X_{\beta_2} E^2 \,\cap\, X_{\beta_3} E^3 \,\cap\, \cdots \,\cap\, X_{\beta_s} E^s\,.$$

This completes the proof of correctness. □

4. The Performance of the Implementation

The Littlewood-Richardson homotopy algorithm has two implementations. One is in the interpreted language of `Macaulay2` [6] using its `NumericalAlgebraicGeometry` package [16], and the other is compiled code and uses the Polynomial Homotopy Continuation package `PHCpack` [32]. These implementations, as well as implementations of the Pieri Homotopy algorithm [11, 12] may be called from the `NumericalSchubertCalculus` package of `Macaulay2`. An introduction to its capabilities and use is given in [17]. This software is free and open source, available on `github` with the compiled version accessible to the Python programmer via `phcpy` [34].

Table 2 gives a selection of the Schubert problems this software is able to solve. These timings (in seconds) compare the performance of the two implementations of Algorithm 2

Grassmannian	Schubert Problem	d	Interpreted	Compiled
$\mathrm{Gr}(2,7)$	$[5,7]^{10}$	42	249.58	1.3652
$\mathrm{Gr}(2,8)$	$[5,8]^{6}$	15	104.04	0.7135
$\mathrm{Gr}(2,9)$	$[6,9]^{7}$	36	455.93	3.4541
$\mathrm{Gr}(2,10)$	$[7,10]^{7}$	91	1899.54	17.3442
$\mathrm{Gr}(3,6)$	$[3,5,6]^{9}$	42	148.65	1.6758
$\mathrm{Gr}(3,7)$	$[4,6,7]^{10}[3,6,7]$	252	2040.51	28.5882
$\mathrm{Gr}(3,8)$	$[4,6,8]^{5}$	32	140.64	8.1716
$\mathrm{Gr}(4,8)$	$[3,4,7,8]^{4}$	6	29.79	5.7789
$\mathrm{Gr}(4,8)$	$[3,6,7,8]^{6}[3,4,7,8]$	50	637.15	27.4836
$\mathrm{Gr}(4,8)$	$[4,6,7,8]^{8}[3,4,7,8]^{2}$	220	3736.61	55.8480

TABLE 2. Timings of Schubert problems

on the same random instance of the problem. These were computed on a Macbook Air with a dual-core Intel Core i5 1.6GHz processor. Here, the exponents indicate repeated brackets.

The compiled implementation is both faster and more robust. Table 3 shows some Schubert problems it can compute, and their timings in h:m:s format. These were computed

Grassmannian	Schubert Problem	d	Time
$\mathrm{Gr}(3,9)$	$[6,8,9]^{14}[5,8,9]^{2}$	30459	59:11:50
$\mathrm{Gr}(4,8)$	$[4,6,7,8]^{16}$	24024	34:09:46
$\mathrm{Gr}(4,9)$	$[5,7,8,9]^{8}[4,6,8,9]^{4}$	25142	293:02:54
$\mathrm{Gr}(5,10)$	$[4,6,8,9,10]^{5}[3,6,7,9,10]^{2}$	8860	216:03:54

TABLE 3. Timings of Schubert problems

on a single processor of a server with four Six-Core AMD Opteron(tm) 8435 processors, each with an 800MHz clock speed, and 64GB memory.

REFERENCES

1. G. Bresler, D. Cartwright, and D. Tse, *Feasibility of interference alignment for the MIMO interference channel*, IEEE Trans. Inform. Theory **60** (2014), no. 9, 5573–5586.
2. C.I. Byrnes, *Pole assignment by output feedback*, Three Decades of Mathematical Systems Theory (H. Nijmeijer and J. M. Schumacher, eds.), Lecture Notes in Control and Inform. Sci., vol. 135, Springer-Verlag, Berlin, 1989, pp. 31–78.
3. A. Eremenko and A. Gabrielov, *Pole placement by static output feedback for generic linear systems*, SIAM Journal on Control and Optimization **41** (2002), no. 1, 303–312.

4. W. Fulton, *Young tableaux*, London Mathematical Society Student Texts, vol. 35, Cambridge University Press, Cambridge, 1997.
5. L.D. García-Puente, N. Hein, C. Hillar, A. Martín del Campo, J. Ruffo, F. Sottile, and Z. Teitler, *The Secant conjecture in the real Schubert calculus*, Experimental Mathematics **21** (2012), no. 3, 252–265.
6. D.R. Grayson and M.E. Stillman, *Macaulay2, a software system for research in algebraic geometry*, Available at `http://www.math.uiuc.edu/Macaulay2/`.
7. J.D. Hauenstein, N. Hein, and F. Sottile, *A primal-dual formulation for certifiable computations in Schubert calculus*, Found. Comput. Math. **16** (2016), no. 4, 941–963.
8. J.D. Hauenstein, M. Safey El Din, É. Schost, and T.X. Vu, *Solving determinantal systems using homotopy techniques*, `arXiv:1802.10409`, 2018.
9. N. Hein, C. Hillar, and F. Sottile, *Lower bounds in real Schubert calculus*, São Paulo Journal of Mathematics **7** (2013), no. 1, 33–58.
10. N. Hein and F. Sottile, *A lifted square formulation for certifiable Schubert calculus*, Journal of Symbolic Compututation **79** (2017), no. part 3, 594–608.
11. B. Huber, F. Sottile, and B. Sturmfels, *Numerical Schubert calculus*, Journal of Symbolic Computation **26** (1998), no. 6, 767 – 788.
12. B. Huber and J. Verschelde, *Pieri homotopies for problems in enumerative geometry applied to pole placement in linear systems control*, SIAM J. Control and Optimization **38** (2000), no. 4, 1265–1287.
13. S.W. Kim, C.J. Boo, S. Kim, and H.-C. Kim, *Stable controller design of MIMO systems in real Grassmann space*, International J. of Control, Automation and Systems **10** (2012), no. 2, 213–226.
14. S.L. Kleiman, *The transversality of a general translate*, Compositio Mathematica **28** (1974), 287–297.
15. S.L. Kleiman and D. Laksov, *Schubert calculus*, Amer. Math. Monthly **79** (1972), no. 10, 1061–1082.
16. A. Leykin, *Numerical Algebraic Geometry*, The Journal of Software for Algebra and Geometry **3** (2011), 5–10, Available at `http://j-sag.org/volume3.html`.
17. A. Leykin, A. Martín del Campo, F. Sottile, R. Vakil, and J. Verschelde, *Software for Numerical Schubert Calculus*, in preparation, 2020.
18. A. Leykin and F. Sottile, *Galois groups of Schubert problems via homotopy computation*, Mathematics of Computation **78** (2009), no. 267, 1749–1765.
19. T. Y. Li, Tim Sauer, and J. A. Yorke, *The cheater's homotopy: an efficient procedure for solving systems of polynomial equations*, SIAM Journal on Numerical Analysis **26** (1989), no. 5, 1241–1251.
20. T.Y. Li, X. Wang, and M. Wu, *Numerical Schubert calculus by the Pieri homotopy algorithm*, SIAM Journal on Numerical Analysis **40** (2002), no. 2, 578–600.
21. A. Martín del Campo, F. Sottile, and R. Williams, *Classification of Schubert Galois groups in Gr(4,9)*, `arXiv.org/1902.06809`, 2019.
22. A. Martín del Campo and F. Sottile, *Experimentation in the Schubert calculus*, Schubert Calculus—Osaka 2012 (H. Naruse, T. Ikeda, M. Masuda, and T. Tanisaki, eds.), Advanced Studies in Pure Mathematics, vol. 71, Mathematical Society of Japan, 2016.
23. A. Morgan, *Solving polynomial systems using continuation for engineering and scientific problems*, Classics in Applied Mathematics, vol. 57, SIAM, 2009.
24. A. P. Morgan and A. J. Sommese, *Coefficient-parameter polynomial continuation*, Appl. Math. Comput. **29** (1989), no. 2, part II, 123–160.
25. F. Sottile, *Pieri's formula via explicit rational equivalence*, Canadian Journal of Mathematics. Journal Canadien de Mathématiques **49** (1997), no. 6, 1281–1298.
26. ———, *Real Schubert calculus: polynomial systems and a conjecture of Shapiro and Shapiro*, Experimental Mathematics **9** (2000), no. 2, 161–182.
27. ———, *Real solutions to equations from geometry*, University Lecture Series, vol. 57, American Mathematical Society, Providence, RI, 2011.
28. F. Sottile, R. Vakil, and J. Verschelde, *Solving Schubert problems with Littlewood-Richardson homotopies*, ISSAC 2010—Proceedings of the 2010 International Symposium on Symbolic and Algebraic Computation, ACM, New York, 2010, pp. 179–186.

29. F. Sottile and J. White, *Double transitivity of Galois groups in Schubert calculus of Grassmannians*, Algebraic Geometry **2** (2015), no. 4, 422–445.
30. R. Vakil, *A geometric Littlewood-Richardson rule*, Annals of Mathematics. Second Series **164** (2006), no. 2, 371–421, Appendix A written with A. Knutson.
31. ———, *Schubert induction*, Annals of Mathematics. Second Series **164** (2006), no. 2, 489–512.
32. J. Verschelde, *Algorithm 795: PHCpack: A general-purpose solver for polynomial systems by homotopy continuation*, ACM Transactions on Mathematical Software **25** (1999), no. 2, 251–276.
33. ———, *Numerical evidence for a conjecture in real algebraic geometry*, Experimental Mathematics **9** (2000), no. 2, 183–196.
34. ———, *Moderizing PHCpack through phcpy*, Proceedings of the 6th European Conference on Python in Science (EuroSciPy 2013) (P. de Buyl and N. Varoquaux, eds.), 2014, pp. 71–76.
35. J. Verschelde and Y. Wang, *Computing feedback laws for linear systems with a parallel Pieri homotopy*, Proceedings of the 2004 International Conference on Parallel Processing Workshops, ICPPW'04, 2004, pp. 222–229.

School of Mathematics, Georgia Institute of Technology, 686 Cherry Street, Atlanta, GA 30332-0160, USA
E-mail address: leykin@math.gatech.edu
URL: http://people.math.gatech.edu/~aleykin3/

Abraham Martín del Campo, Centro de Investigación en Matemáticas, A.C., Jalisco S/N, Col. Valenciana, 36023, Guanajuato, Gto., México
E-mail address: abraham.mc@cimat.mx
URL: http://personal.cimat.mx:8181/~abraham.mc/

Frank Sottile, Department of Mathematics, Texas A&M University, College Station, Texas 77843, USA
E-mail address: sottile@math.tamu.edu
URL: www.math.tamu.edu/~sottile

Ravi Vakil, Department of Mathematics, Stanford University, Stanford, CA 94305 USA
E-mail address: vakil@math.stanford.edu
URL: http://math.stanford.edu/~vakil

Jan Verschelde, Dept of Math, Stat, and CS, University of Illinois at Chicago, 851 South Morgan (M/C 249), Chicago, IL 60607 USA
E-mail address: jan@math.uic.edu
URL: http://www.math.uic.edu/~jan